ATTORNEY DOCKET NO. 23016.0002US
PATENT

IN THE UNITED STATES PATENT AND TRADEMARK OFFICE

In re Application of	)	
	)	
Wynick, David	)	Art Unit: 1647
	)	
Application No. 09/230,463	)	Examiner: Gucker, S.
	)	
Filing Date: January 22, 1999	)	Confirmation No. 4323
	)	
For: "GALANIN"	)	

DECLARATION UNDER 37 C.F.R. § 1.132

1. I am Professor of Molecular Medicine at the Henry Wellcome Laboratories for Integrative Neuroscience and Endocrinology, the University of Bristol, United Kingdom.

2. I am the inventor named for US patent application no. 09/230,463.

3. I have measured the length of 21 nerve roots (i.e. the part of the nerve that connects the cell bodies of the DRG to the dorsal horn of the spinal cord) which were harvested from the lumbar region of 5 female Sprague-Dawley rats weighing 200-250g. The length of the nerve root was then measured using a calibrated graticule and a dissecting microscope and the mean length was found to be 18.5±0.9 mm (see Exhibit A, attached).

4. This figure is in good agreement with the findings of Michael et al. (Michael et al. (1997) J. Neurosci. **17** 8476-8490) who found the nerve root of adult male Wistar rats (200-400g body weight) to be 17 mm in length. Similarly, Baba et al. (Baba et al. (1999) J. Neurosci. **2** 859-867) found the dorsal root to be between 18-20 mm in length in adult male Sprague-Dawley rats weighing 300-350g.

5. I further declare that all statements made herein of my own knowledge and belief are true and that all statements made on information and belief are believed to be true, and further, that the statements are made with the knowledge that willful false statements are

punishable by fine or imprisonment, or both, under section 1001 of Title 18 of the United States Code, and that such willful false statements may jeopardize the validity of the application or any patent issuing thereon.

Date: 7th June 2005

Professor David Wynick

EXHIBIT A

Mean length ± SEM (mm) of 21 spinal nerve roots harvested from the lumbar region of 5 female Sprague-Dawley rats weighing 200-250g. The length of the spinal nerve root was measured using a calibrated graticule and a dissecting microscope.

Length (mm)
18
19
20
18
18
18
17
19
19
17
18
20
18
20
18
19
18
20
19
18
18

Mean: 18.5±0.9

The Journal of Neuroscience, January 15, 1999, 19(2):859–867

Peripheral Inflammation Facilitates Aβ Fiber-Mediated Synaptic Input to the Substantia Gelatinosa of the Adult Rat Spinal Cord

Hiroshi Baba, Timothy P. Doubell, and Clifford J. Woolf

Neural Plasticity Research Group, Department of Anesthesia and Critical Care, Massachusetts General Hospital and Harvard Medical School, Boston, Massachusetts 02129

Whole-cell patch-clamp recordings were made from substantia gelatinosa (SG) neurons in thick adult rat transverse spinal cord slices with attached dorsal roots to study changes in fast synaptic transmission induced by peripheral inflammation. In slices from naive rats, primary afferent stimulation at Aβ fiber intensity elicited polysynaptic EPSCs in only 14 of 57 (25%) SG neurons. In contrast, Aβ fiber stimulation evoked polysynaptic EPSCs in 39 of 62 (63%) SG neurons recorded in slices from rats inflamed by an intraplantar injection of complete Freund's adjuvant (CFA) 48 hr earlier ($p < 0.001$). Although the peripheral inflammation had no significant effect on the threshold and conduction velocities of Aβ, Aδ, and C fibers recorded in dorsal roots, the mean threshold intensity for eliciting EPSCs was significantly lower in cells recorded from rats with inflammation (naive: 33.2 ± 15.1 μA, $n = 57$; inflamed: 22.8 ± 11.3 μA, $n = 62$, $p < 0.001$), and the mean latency of EPSCs elicited by Aβ fiber stimulation in CFA-treated rats was significantly shorter than that recorded from naive rats (3.3 ± 1.8 msec, $n = 36$ vs 6.0 ± 3.5 msec, $n = 12$; $p = 0.010$). Aβ fiber stimulation evoked polysynaptic IPSCs in 4 of 25 (16%) cells recorded from naive rat preparations and 14 of 26 (54%) SG neurons from CFA-treated rats ($p < 0.001$). The mean threshold intensity for IPSCs was also significantly lower in CFA-treated rats (naive: 32.5 ± 15.7 μA, $n = 25$; inflamed: 21.9 ± 9.9 μA, $n = 26$, $p = 0.013$). The facilitation of Aβ fiber-mediated input into the substantia gelatinosa after peripheral inflammation may contribute to altered sensory processing.

Key words: inflammation; pain; dorsal horn; synaptic transmission; neural plasticity; substantia gelatinosa

Peripheral tissue inflammation characteristically leads to increased pain sensitivity. This is the consequence both of a peripheral sensitization of high-threshold Aδ and C nociceptor terminals on exposure to inflammatory mediators (Levine and Taiwo, 1994) and to a central facilitation of synaptic input into the dorsal horn of the spinal cord; central sensitization (Woolf, 1983; Torebjork et al., 1992). Central sensitization is initiated in noninflamed animals by brief C-fiber inputs and manifests as a modification in the receptive field properties of dorsal horn neurons caused by the recruitment of subthreshold inputs (Woolf and King, 1990), and includes the transformation of nociceptive-specific cells into multireceptive cells with a low-threshold Aβ fiber input (Simone et al., 1989; Woolf et al., 1994). In human volunteers, central sensitization induced by activation of C-fibers with chemical irritants includes the generation of a tactile pain mediated by Aβ fibers (Torebjork et al., 1992; Koltzenburg et al., 1994). In *in vitro* neonatal spinal cord preparations, repetitive brief C-fiber stimulation produces an NMDA receptor-mediated heterosynaptic facilitation of Aβ fiber inputs to deep dorsal horn and ventral horn spinal neurons (Thompson et al., 1990, 1993).

Central sensitization is likely to contribute substantially to the hypersensitivity associated with experimental inflammation as a consequence of C-fiber input from spontaneously active C-fibers or augmented peripheral activation of sensitized C-fibers. Another mechanism may, however, participate in alterations in synaptic efficacy during inflammation, a change in the synaptic drive generated by Aβ sensory neurons innervating the inflamed area. In adjuvant-inflamed but not naive rats, for example, the hamstring flexor withdrawal reflex is progressively sensitized by repetitive light mechanical stimuli applied to the inflamed tissue (progressive tactile hypersensitivity), which can be mimicked by Aβ fiber electrical stimulation (Ma and Woolf, 1996a). Aβ fiber input in inflamed animals also generates an action potential afterdischarge in dorsal horn neurons, something only Aδ and C-fibers normally evoke (Neumann et al., 1996). Finally, Aβ fiber-mediated ventral root potentials recorded from an *in vitro* spinal cord preparation from inflamed neonatal rats, show windup, a phenomenon normally only associated with C-fibers (Thompson et al., 1994). One explanation for these changes in the central action of Aβ fibers after inflammation may be the novel expression of substance P and other synaptic modulators in some of these fibers (Neumann et al., 1996), which could result in synaptic events typical of C-fibers being generated by Aβ fibers.

The central changes involved in inflammation may result in the facilitation of Aβ fiber-mediated synaptic input to neurons in the superficial dorsal horn, especially lamina II (substantia gelatinosa, SG). The direct primary afferent input into the SG is predominantly Aδ and C fiber nociceptors (Willis and Coggeshall, 1991), and the novel recruitment of low-threshold Aβ-evoked synaptic potentials in these neurons might alter sensory processing sufficiently to contribute to the abnormal hypersensitivity typical of inflammation. We have now investigated, using an *in vitro* adult

Received Aug. 3, 1998; revised Oct. 22, 1998; accepted Nov. 3, 1998.

Supported by the Human Frontier Science Program (RG73/96) and the Wellcome Trust (039631).

Correspondence should be addressed to Dr. Hiroshi Baba, Neural Plasticity Research Group, Department of Anesthesia, Massachusetts General Hospital and Harvard Medical School, MGH-East 4th Floor, 149 13th Street, Charlestown, MA 02129.

Dr Doubell's present address: University Laboratory of Physiology, University of Oxford, Oxford, OX 1 3PT UK.

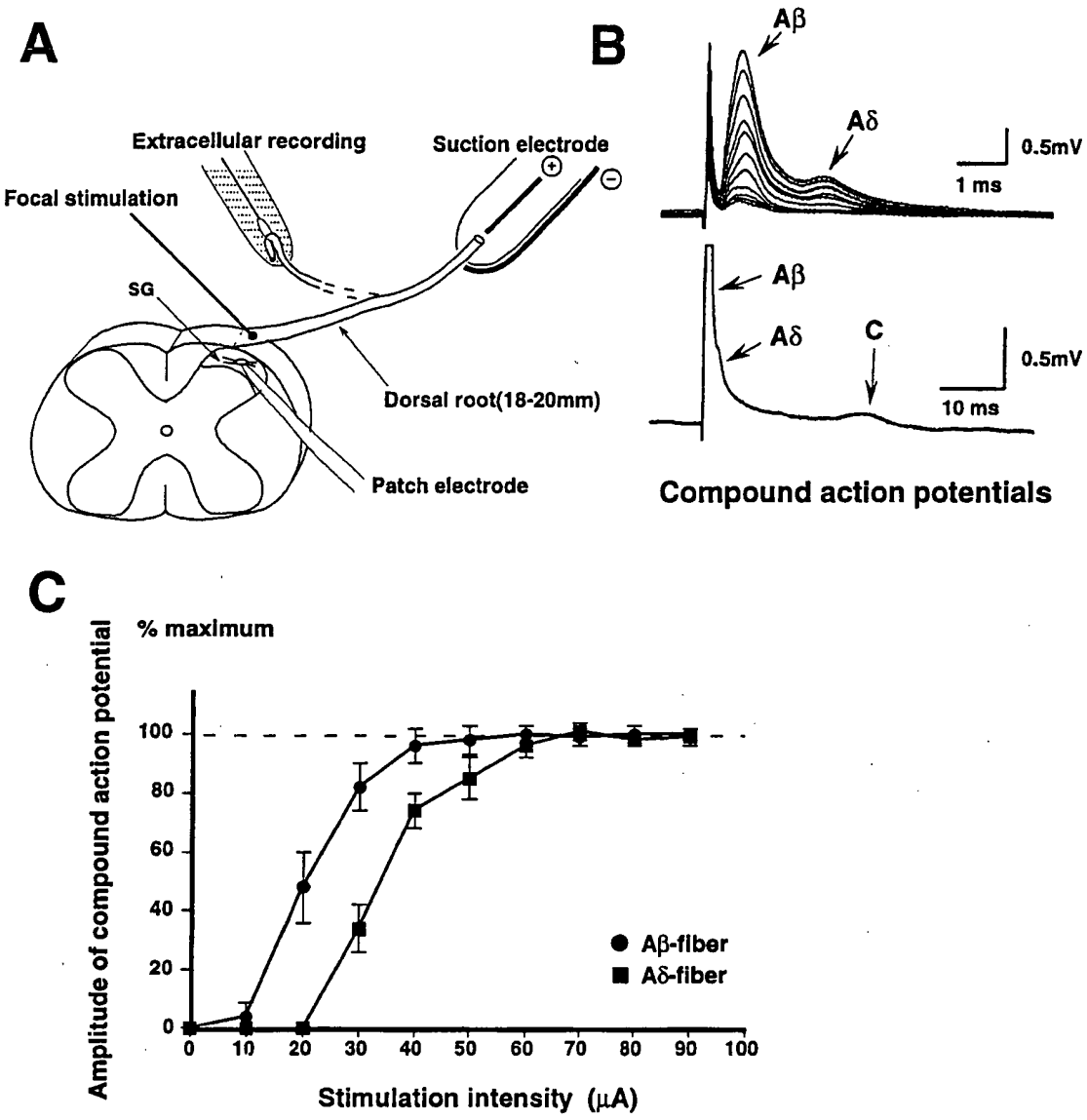

Figure 1. *A*, Schematic diagram of the experimental setup. Extracellular recordings were made from dorsal roots, and whole-cell patch-clamp recordings were made from SG neurons in adult rat spinal cord transverse slices with a long attached dorsal root. *B*, Representative extracellular recording of compound action potentials evoked at graded stimulus intensities (*top*, 12–50 μA; *bottom*, 300 μA). The threshold intensities for Aβ, Aδ, and C fibers were 12, 23, and 230 μA, respectively. The stimulus duration for Aβ and Aδ was 0.05 msec and for C fibers was 0.5 msec. Calculated conduction velocities for Aβ, Aδ, and C fibers were 27.3, 8.5, and 0.8 m/sec, respectively. *C*, The stimulus–response relationship of Aβ and Aδ compound action potentials ($n = 5$).

spinal cord preparation, the effect of inflammation on Aβ fiber-mediated fast synaptic responses in the SG.

MATERIALS AND METHODS

The methods for inducing inflammation, obtaining adult rat spinal cord slices, and blind whole-cell patch-clamp recordings from SG neurons have been described in detail previously (Yoshimura and Jessell, 1989; Yoshimura and Nishi, 1993; Ma and Woolf, 1996a). Briefly, inflammation was induced by an intraplantar injection of complete Freund's adjuvant (CFA; Sigma, St. Louis, MO; 100 μl) into the left hindpaw of adult male Sprague Dawley rats (10–11 weeks, 300–350 gm) under halothane (2.5%) anesthesia, producing an area of erythema, edema, and tenderness restricted to the hindpaw (Stein et al., 1988). Naive noninflamed animals or rats 48 hr after CFA injection were terminally anesthetized with urethane (1.5–2.0 gm/kg, i.p.), and the lumbosacral spinal cord was removed. The isolated spinal cord was then placed in preoxygenated cold Krebs' solution (2–4°C). After removal of the dura mater, all ventral and dorsal roots, except the L5 dorsal root on the left side, were cut, and the pia-arachnoid was removed. The spinal cord was placed in a shallow groove formed in an agar block and glued to the bottom of a microslicer stage with cyanoacrylate adhesive and held in place by the agar block. The spinal cord was immersed in cold Krebs' solution, and a 600-μm-thick transverse slice with attached dorsal root was cut on a vibrating microslicer (model DTK1500; Dosaka Co. Ltd., Kyoto, Japan). The spinal cord slice was then placed on a nylon mesh in the recording chamber and held in place by a titanium electron microscopy grid supported by a silver wire loop. The slice was perfused with Krebs' solution (15 ml/min) saturated with 95% O_2 and 5% CO_2 at 36 ± 1°C. The Krebs' solution contained (in mM): NaCl 117, KCl 3.6, $CaCl_2$ 2.5, $MgCl_2$ 1.2, NaH_2PO_4 1.2, $NaHCO_3$ 25, and glucose 11. The length of preserved L5 dorsal root from the cathode of the suction electrode to the dorsal root entry zone was adjusted to 18–20 mm by cutting its distal end. Orthodromic stimulation of the dorsal root was performed with a suction electrode (Fig. 1*A*) using a constant-current stimulator (Neurolog). The

Table 1. Compound action potential

	Threshold (μA)			Conduction velocity (m/sec)		
	Aβ	Aδ	C	Aβ	Aδ	C
Naive (n = 12)	13.3 ± 2.7	24.7 ± 1.9	217.9 ± 76.9	27.0 ± 3.7	8.0 ± 1.2	0.8 ± 0.1
Inflamed (n = 14)	12.6 ± 2.7	25.4 ± 2.2	198.0 ± 77.3	26.0 ± 4.3	8.1 ± 1.1	0.9 ± 0.1

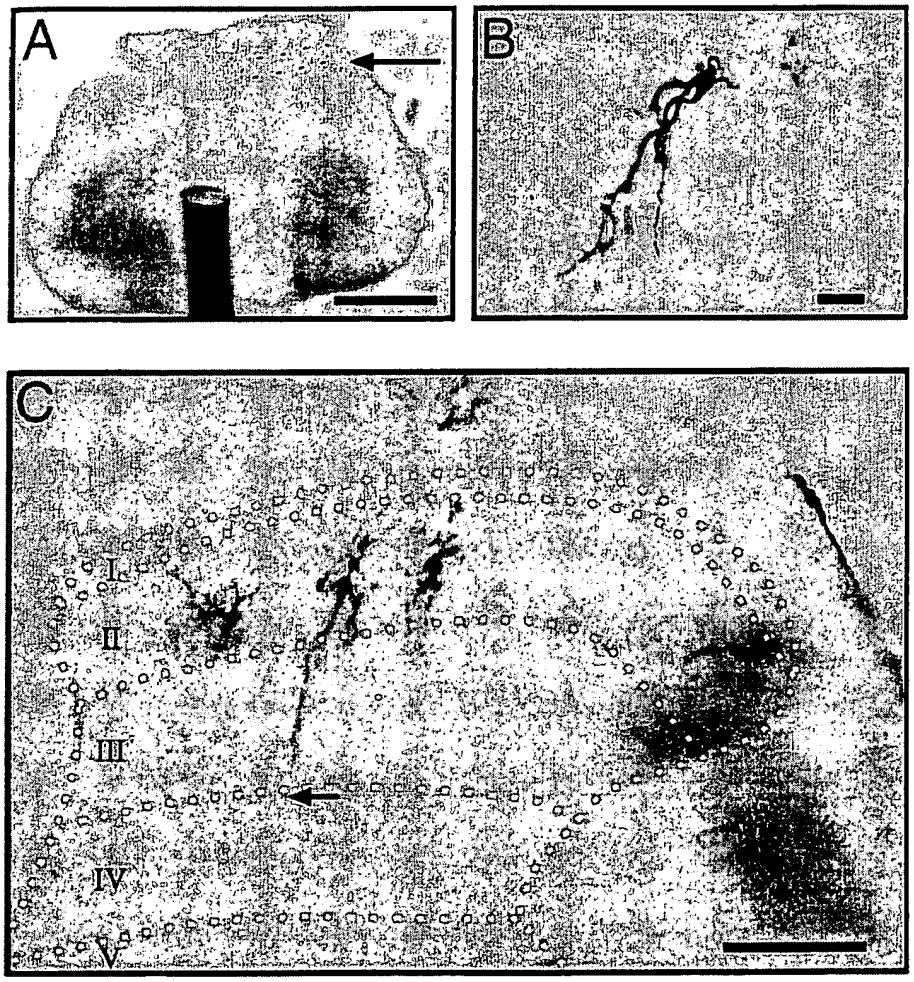

Figure 2. Identification of SG and SG neurons in the transverse spinal cord slices. *A*, Photomicrograph of the slice preparation from naive rat showing that the SG can be identified as a translucent pale area in the superficial dorsal horn (*dotted area*) enabling targeting of the recording electrode to the this region. Scale bar, 600 μm. *B*, A representative SG neuron injected with Neurobiotin. Scale bar, 20 μm. *C*, A low-power photomicrograph of a slice from naive rat showing SG neurons filled with Neurobiotin. Note all neurons lie within the middle third of the dorsoventral plane of SG and have the features typical of stalk cells. The dendrites of some cells extend ventrally into deeper laminae as indicated by the *arrow*. Scale bar, 150 μm.

stimulus intensity necessary to activate Aα/β, Aδ, and C fibers and the afferent fiber conduction velocity was determined by extracellular recording of compound action potentials from the dorsal root near the dorsal root entry zone in each experiment. The minimum stimulus intensities and duration to activate Aα/β, Aδ, and C fibers were ~10 μA (0.05 msec), 25 μA (0.05 msec), and 200 μA (0.5 msec), respectively (Fig. 1*A*,*B*; Table 1). In some experiments, focal stimulation was performed with a monopolar silver wire electrode (50 μm diameter), insulated except at the tip, positioned just distal to the dorsal root entry zone to estimate conduction velocity of the fibers responsible for particular synaptic responses.

Blind whole-cell patch-clamp recordings were made from neurons located in SG (Figs. 1*A*, 2*A*). With a light source directed under the slice, the SG, because of its relative lack of myelin is readily identifiable as a distinct translucent region in the superficial dorsal horn (Fig. 2*A*) (Yoshimura and Nishi, 1993). The recording electrodes were positioned, in all cases, under direct visual control into the middle third of SG, identified as above, in the dorsoventral plane and within its medial half in the mediolateral plane. The location of recorded neurons was confirmed in selected instances by the intrasomatic injection of Neurobiotin (0.3%; Vector Laboratories, Burlingame, CA).

Two pipette solutions were used in this study, the first, which was used in most cases with TEA and Cs, contained (in mM): Cs-sulfate 110, $CaCl_2$ 0.5, $MgCl_2$ 2, EGTA 5, HEPES 5, TEA 5, and ATP-Mg salt 5, and the second, without Cs and TEA, contained (in mM): potassium gluconate 135, KCl 5, $CaCl_2$ 0.5, $MgCl_2$ 2, EGTA 5, HEPES 5, ATP-Mg salt 5, and Na-GTP 0.5. The resistance of a typical patch pipette was 5–10 MΩ. Voltage-clamped neurons were held at a membrane potential of −70 mV for recording EPSCs and at 0 mV for recording IPSCs. At 0 mV, only IPSCs produce upward deflections (Baba et al., 1998), because the reversal potentials of EPSCs are ~0 mV (Yoshimura and Jessell, 1990).

Membrane currents were amplified with an Axopatch 200A amplifier (Axon Instruments, Foster City, CA) in voltage-clamp mode. Signals were filtered at 2 kHz and digitized at 5 kHz. Data were analyzed using pClamp 6 (Axon Instruments). Membrane potential and input resistance were measured shortly after establishing whole-cell clamp.

In preliminary experiments in 15 SG cells recorded in the absence of TEA/Cs in the pipette solution, no indication of an augmentation of K^+ channel-associated slow synaptic currents after inflammation was detected. Because the Cs/TEA-containing pipette solution, although obscuring such K^+ currents, improved space clamp and the capacity to

Table 2. Criteria for the classification of synaptic responses

Classification	Threshold	Monosynaptic (Fixed latency)	Polysynaptic (Variable latency)	Latency
Aβ mono	<50 μA	+		<2.2 msec
Aβ poly	<25 μA		+	
Aδ mono	>25 μA	+		2.2–10 msec
Aβ/Aδ poly	25–50 μA		+	
Aδ poly	>50 μA		+	
C mono	>200 μA	+		20–40 msec

record IPSCs, we used it to record the fast A fiber-mediated synaptic responses that were under investigation in this study.

Statistical analysis on differences in threshold and latencies of neurons recorded in control and inflamed tissue was performed using a nested ANOVA and on the proportions of cells with particular synaptic response by logistic regression with GEE techniques. Results presented are mean ± SD.

RESULTS

Identification of SG neurons

The neurons recovered after intrasomatic injection of Neurobiotin showed that targeting the electrode into the SG resulted in recordings from neurons with cell bodies in lamina II in all cases (n = 21) (Fig. 2*C*). These cells had, moreover, morphological features and cell body diameters similar to those described previously in the rat SG using Golgi (Beal and Bicknell, 1985) and intracellular HRP (Woolf and Fitzgerald, 1983)-labeling techniques and included stalked and islet cells, the most common cell types of the region. A distinctive feature in several cells was dendrites extending ventrally into the deeper laminae of the dorsal horn (Fig. 2*C*).

Membrane properties and spontaneous synaptic responses of SG neurons

The average membrane potentials of SG neurons recorded from naive preparations were −64.5 ± 6.2 mV (n = 21) and, in animals with inflammation they were −65.7 ± 7.4 mV (n = 25). Mean input resistance was 746 ± 357 MΩ (n = 11) in naive and 834 ± 453 MΩ (n = 14) in cells from inflamed animals, suggesting that similar sized cells were recorded in both cases. The frequency of spontaneous EPSCs was 35.9 ± 17.6 Hz (n = 12) from naive and 32.1 ± 24.1 Hz (n = 15) from cells recorded in preparations from inflamed animals. The frequency of spontaneous IPSCs was 23.2 ± 13.0 Hz (n = 5) in naive and 17.9 ± 10.7 Hz (n = 6) in preparations from inflamed animals. No significant differences in these passive and active membrane characteristics were detected between neurons recorded from slices prepared from naive and CFA-treated rats.

Primary afferent threshold and conduction velocity

Primary afferents could be divided into three distinct groups, corresponding to Aα/β, Aδ, and C fibers, on the basis of the threshold and conduction velocity of compound action potentials recorded extracellularly on the dorsal root (Fig. 1*B*). Figure 1*C* illustrates the stimulus response functions of Aα/β fiber and Aδ fiber volleys in the dorsal root at a pulse width of 50 μsec and shows that at <25 μA, only an Aβ wave is detectable with a maximum amplitude at 50 μA. Any new response elicited above 50 μA is likely to be, therefore, Aδ-mediated. It is possible that at thresholds below that necessary to detect an Aδ wave, a few single Aδ fibers may be activated. Table 1 shows that the stimulation thresholds and conduction velocities for the Aα/β, Aδ, and C fibers recorded in preparations from naive and rats with an inflamed hindpaw did not differ significantly. The values obtained for threshold and conduction velocity are in agreement with those found in earlier studies *in vivo* (Lynn and Carpenter, 1982; Harper and Lawson, 1985; Villiere and McLachlan, 1996).

Synaptic responses in SG neurons

Whole-cell patch-clamp recordings were made from 57 SG neurons in slices prepared from naive rats (n = 12) and 62 neurons in slices from rats inflamed 48 hr before with CFA (n = 14). All SG neurons recorded responded to orthodromic dorsal root stimulation. Table 2 shows the criteria for the classification of synaptic responses into Aβ or Aδ monosynaptic or polysynaptic in terms of threshold, response to repetitive inputs, and latency. Identification of EPSCs as monosynaptic was based on a constant latency and absence of failures with repetitive stimulation at a frequency of 20 Hz (Fig. 3*A*, *middle*, *bottom*) (Yoshimura and Jessell, 1989). Polysynaptic EPSCs, in contrast, had variable latencies and showed failures at 20 Hz (Fig. 3*A*, *top*; see Fig. 6*B*). At stimulus thresholds between 25 and 50 μA, it was not possible because of the stimulus response profile of the afferent volleys (Fig. 1*C*) to differentiate unambiguously any polysynaptic responses elicited into Aβ or Aδ, and we have classified these, therefore, as Aβ/Aδ (Table 2).

Most SG neurons recorded from naive rat slices exhibited either monosynaptic or polysynaptic Aδ fiber-mediated EPSCs. A small proportion of cells (25%) from the control preparations had Aβ fiber-mediated polysynaptic input, but none had a monosynaptic Aβ fiber input (Table 3), in agreement with earlier findings (Yoshimura and Nishi, 1993). No cells with an input exclusively from C-fibers were found. Polysynaptic IPSCs were recorded in some neurons at a holding membrane potential of 0 mV (Fig. 3*B*) and were mediated by $GABA_A$ and/or glycine receptors, as evidenced by the antagonism with bicuculline and strychnine (Fig. 3*C*). As for the EPSCs, the IPSCs in most SG neurons in naive rats were mediated by Aδ fibers, confirming the previous study (Yoshimura and Nishi, 1995), and only a small proportion of cells had Aβ fiber-mediated polysynaptic IPSCs (16%) (Table 3).

Synaptic responses in SG neurons recorded from rats with an inflamed hindpaw

In contrast to the naive situation, SG neurons recorded from slices obtained from rats with an inflamed hindpaw exhibited Aβ fiber-evoked polysynaptic EPSCs in the majority of cases (39 of 62; 63%; Table 3) ($p < 0.001$). No Aβ fiber-mediated monosynaptic EPSCs could be detected in these rats. Figure 4*A* shows the distribution of the minimum stimulus intensity threshold for eliciting EPSCs in slices from naive and rats with

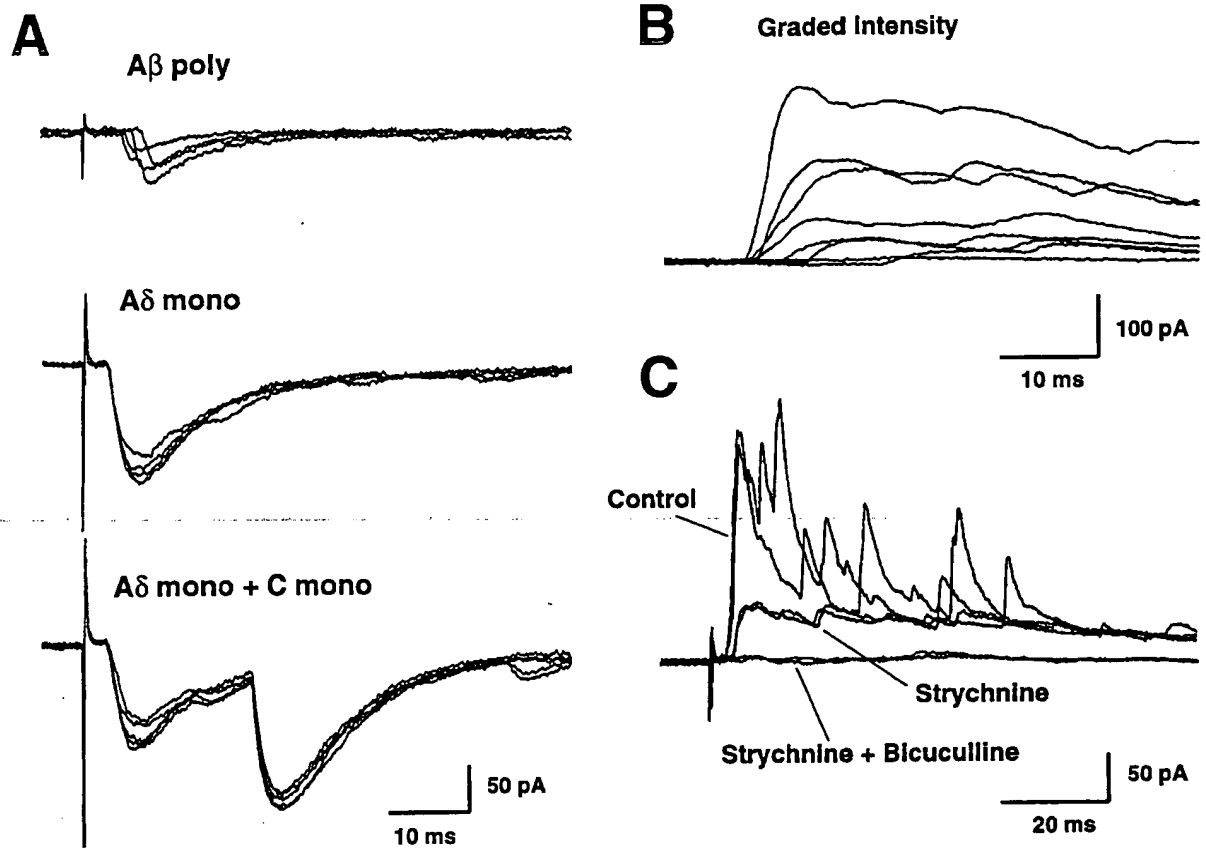

Figure 3. *A*, The *top*, *middle*, and *bottom* show respectively, EPSCs evoked by Aβ (14–20 μA, 0.05 msec), Aδ (32–50 μA, 0.05 msec), and C (200–500 μA, 0.5 msec) fiber intensities. Four to five traces are superimposed in each panel. *Top*, Aβ fiber-evoked polysynaptic EPSCs. *Middle*, Aδ fiber-evoked monosynaptic EPSCs. *Bottom*, Aδ and C fibers evoked monosynaptic EPSCs. Note that the latencies were constant for the monosynaptic EPSCs and variable in the polysynaptic responses. The above records were obtained from a single neuron. *B*, Polysynaptic IPSCs evoked by graded stimulation. As the intensity was increased from 15 to 40 μA, 0.05 msec, the latency of the IPSC shortened. *C*, The effects of strychnine (2 μM) and bicuculline (20 μM) on IPSCs. Strychnine eliminated the short-latency component of the IPSC, whereas bicuculline reduced the longer latency component.

Table 3. Classification of synaptic responses

	Aβ-mono	Aβ-poly	Aδ-mono	Aβ/Aδ poly	Aδ-poly	C-mono
EPSCs						
Naive (n = 57)	0 (0%)	14 (25%)	15 (26%)	25 (44%)	8 (14%)	8 (14%)
Inflamed (n = 62)	0 (0%)	39 (63%)	12 (19%)	19 (30%)	1 (2%)	6 (10%)
IPSCs						
Naive (n = 25)	0 (0%)	4 (16%)	0 (0%)	19 (76%)	2 (8%)	0 (0%)
Inflamed (n = 26)	0 (0%)	14 (54%)	0 (0%)	12 (46%)	0 (0%)	0 (0%)

inflammation. In slices from CFA-treated rats, the mean threshold intensity was 22.8 ± 11.3 μA, which was significantly lower than that in the naive preparations (33.2 ± 15.1 μA; $p < 0.001$; n = 57 for naive rat and 62 for CFA-treated rats). The threshold in the inflamed preparations is well below that for eliciting Aδ volleys (Fig. 1*C*). This difference cannot be caused by changes in afferent fiber excitability because peripheral inflammation had no significant effect on either the thresholds or the conduction velocities of Aβ, Aδ, and C fibers (Table 1). Figure 5*A* shows the distribution of the latencies of EPSCs evoked at a stimulus intensity of 20 μA, 0.05 msec (above the threshold for Aβ but below the threshold of Aδ fibers). Mean latencies of EPSCs in naive and CFA-treated rats at this stimulus intensity were 6.0 ± 3.5 msec (n = 12) and 3.3 ± 1.8 msec (n = 36), respectively (p = 0.010). In the CFA-treated rats, Aβ fiber-mediated polysynaptic EPSCs with a very short latency (<2.0 msec), which is much shorter than that of Aδ fiber-mediated monosynaptic EPSCs (latency, 2.2–3.5 msec), could be detected (Fig. 5*A*, Fig. 6). These short-latency EPSCs were never recorded in cells from naive animals at this stimulus strength. The conduction velocity calculated by two point stimulation along the length of the dorsal root was in Aβ fiber range (>15 m/sec) (Fig. 6*C*). Stimulation at an intensity of 100 μA 0.05 msec, which is supramaximal for Aβ fibers and above the Aδ threshold (Fig. 5*B*), also resulted in a shorter mean latency of EPSC in inflamed rats (2.6 ± 1.0 msec; n = 60) than

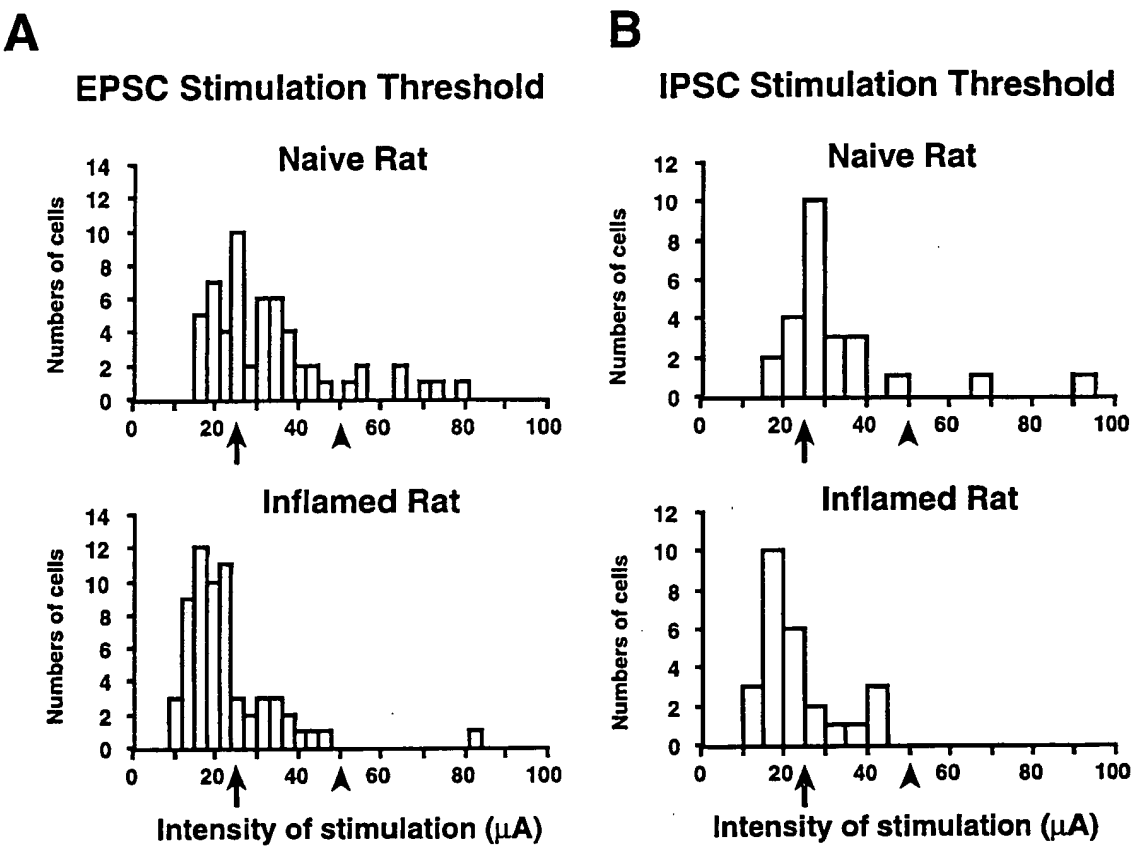

Figure 4. Distribution of the minimum stimulus threshold intensities necessary for eliciting EPSCs and IPSCs in cells recorded in the SG in slices from naive and CFA-treated rats. The mean stimulus threshold intensity required to evoke EPSCs in naive and CFA-treated rats was 33.2 ± 15.1 μA (n = 57) for naive and 22.8 ± 11.3 μA (n = 62) for CFA-treated rats ($p < 0.001$; nested ANOVA). The mean stimulus threshold intensity required to evoke IPSCs in naive and rats with an inflamed hindpaw was 32.5 ± 15.7 μA (n = 25) for naive and 21.9 ± 9.9 μA (n = 26) for the CFA-treated rats (p = 0.013; nested ANOVA). The *arrow* indicates the stimulus intensity at which an Aδ volley begins to be detected, all responses below this value are exclusively Aβ. The *arrowhead* represents the stimulus value at which a maximal Aβ volley is elicited. All responses elicited above this intensity are exclusively Aδ-evoked. For values between the *arrow* and the *arrowhead*, the responses evoked may be Aβ- and/or Aδ-evoked.

in naive rats (3.1 ± 1.1 msec; n = 53; $p < 0.05$). The suprathreshold stimulus also shortened the EPSC latency compared with the submaximal stimulus.

In SG neurons recorded from rats with inflammation, polysynaptic IPSCs were evoked by Aβ fiber intensity stimulation in about half of cells (14 of 26; 54%; Table 3), which is significantly greater than naives ($p < 0.001$). Figure 4*B* shows the distribution of the minimum stimulus intensity threshold for eliciting IPSCs in slices from naive and CFA-treated rats. In slices from rats with an inflamed hindpaw, the mean threshold intensity was 21.9 ± 9.9 μA, which was significantly lower than that in the naive preparations (32.5 ± 15.7 μA; p = 0.013; n = 25 for naive rat and 26 for inflamed group).

DISCUSSION

We have found that a localized peripheral inflammation for 48 hr results in a facilitation of short-latency fast Aβ fiber-mediated polysynaptic EPSCs and IPSCs in SG neurons that receive sensory input from sensory fibers innervating the inflamed area.

Aβ fiber-mediated synaptic input to the SG

There is substantial evidence that the primary function of neurons in the SG is to integrate noxious afferent information carried by the high-threshold Aδ and C fibers that terminate in this region of the superficial dorsal horn (Willis and Coggeshall, 1991). The SG cells, acting as inhibitory and excitatory interneurons, modify the output of projection neurons in both lamina I and the deeper layers of the dorsal horn (Willis and Coggeshall, 1991). The vast majority of SG neurons have high-threshold receptive fields, but an excitation of SG neurons by innocuous mechanical stimuli and Aβ fiber electrical stimulation has been reported in a small number of cells in *in vivo* studies (Kumazawa and Perl, 1978; Bennett et al., 1980; Woolf and Fitzgerald, 1983). Studies in adult spinal cord slices with an attached dorsal root show a similar picture. Although short-latency fast excitatory synaptic responses in SG cells in these preparations have been found to be predominantly mediated by Aδ fibers, Aβ fiber-mediated EPSCs are also detected, but only in a small proportion of SG neurons. These Aβ fiber-mediated EPSCs always have a variable and longer latency than the more common monosynaptic Aδ EPSCs (Yoshimura and Jessell, 1989; Yoshimura and Nishi, 1993). *In vitro* studies with immature young rat spinal cord preparations have not reported Aβ fiber-mediated fast EPSCs, which may reflect developmental changes or technical issues relating to the thickness of the slice and the length of dorsal root available (Bleazard et al., 1994; Randic et al., 1995; Sandkuhler et al., 1997).

Because Aβ fibers do not project directly to SG but to lamina III-VI (Brown, 1981; Woolf, 1987) and because the dendrites of many SG neurons do not leave SG (Light et al., 1979; Bennett et

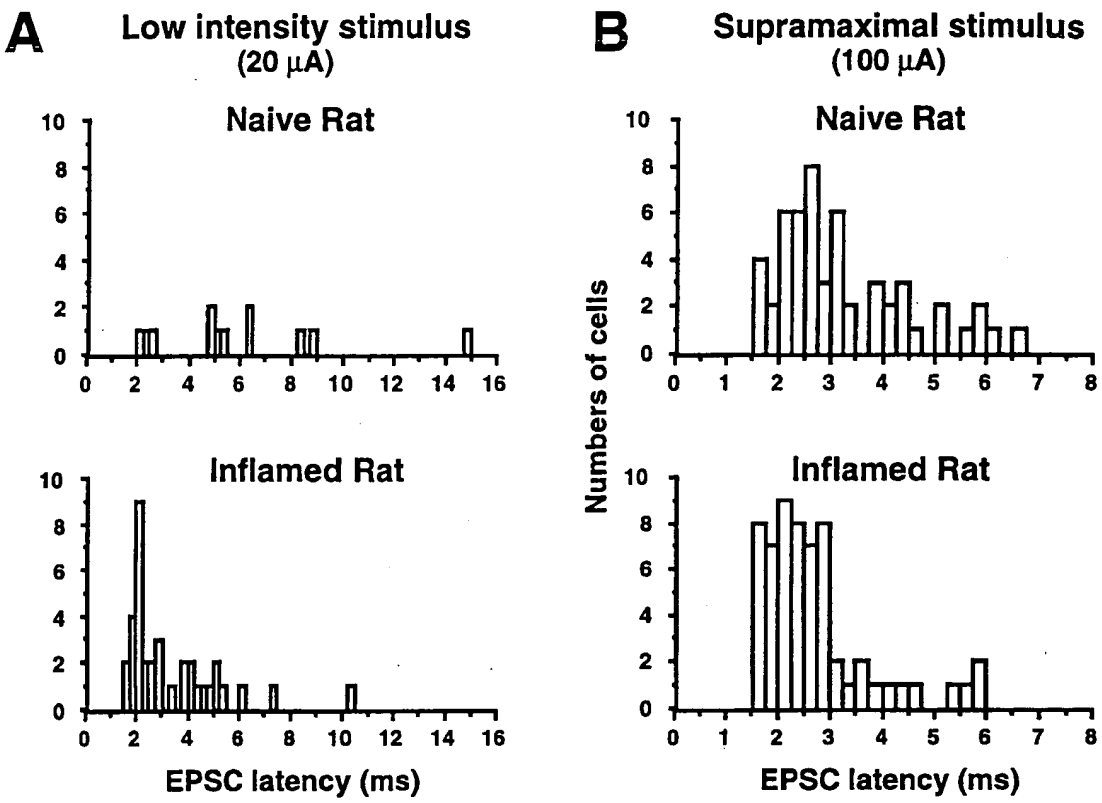

Figure 5. Distribution of the latencies of EPSCs in cells recorded in the SG in slices from naive and CFA-treated rats. *A*, The EPSC latencies evoked by Aβ fiber intensity (20 μA, 0.05 msec, below Aδ fiber threshold) were significantly shortened in the rats with an inflamed hindpaw; 3.3 ± 1.8 msec versus 6.0 ± 3.5 msec ($p = 0.010$; nested ANOVA; $n = 12$ in naive and $n = 36$ in inflamed rats). Aβ fiber-mediated EPSCs with short latencies (<2.0 msec) were only observed in the preparations from rats with an inflamed hindpaw. *B*, Distribution of the latencies of EPSCs evoked by supramaximal Aβ fiber stimulation intensity. Mean latency of EPSCs in CFA-treated rats was 2.6 ± 1.0 msec ($n = 60$), which was significantly shorter than that recorded in naive rats (3.1 ± 1.1 msec; $n = 53$; nested ANOVA; $p < 0.05$).

al., 1980), it has been commonly assumed that all responses to Aβ fiber stimulation must depend on polysynaptic pathways. In support of this is our failure ever to detect an Aβ fiber-evoked monosynaptic EPSC in the SG. However, there are some cells in the SG with dendrites that extend into the deep dorsal horn (Woolf and Fitzgerald, 1983; Fig. 2*C*). The question should be therefore, why, given this potential anatomical substrate for a direct Aβ input to some SG cells, has no such input ever been seen in naive animals or even after inflammation?

Potential mechanisms responsible for the facilitation of Aβ fiber mediated-input into SG after inflammation

There are two possible general mechanisms that could result in the recruitment of fast Aβ-evoked synaptic responses in the SG; a strengthening of pre-existing ineffective or silent synapses or the establishment of novel synapses by a structural alteration in synaptic connectivity. The former is likely to operate after inflammation, and the latter may well contribute to changes after nerve injury (Woolf et al., 1992). A functional change in synaptic connectivity could be caused by presynaptic or postsynaptic alterations, either increasing excitability or reducing inhibition and may operate at the first synapse between the afferent and dorsal horn neurons or on subsequent neurons in the polysynaptic chain that carries the Aβ fiber input to the SG from deep laminae. One example of a presynaptic change in primary afferents that could increase synaptic strength is a shift in transmitter content in A fibers. After inflammation, for example, some Aβ fibers, which are normally not substance P-immunoreactive, begin to express this peptide (Neumann et al., 1996). Aβ fibers also acquire the novel capacity to induce an NK1-mediated windup-like phenomenon (Thompson et al., 1994; Herrero and Cervero, 1996a,b). Inflammation also changes the nature of those peripheral stimuli that can evoke activity-dependent c-fos expression in the dorsal horn from predominantly nociceptors in the naive state (Hunt et al., 1987; Presley et al., 1990) to one that includes Aβ fibers (Ma and Woolf, 1996b). Other mechanisms that may potentially increase synaptic strength include increased transmitter release, increased postsynaptic receptors, reduced uptake or breakdown of transmitters, post-translational changes in receptor function, or alterations in postsynaptic membrane excitability. We found no change in the membrane potential of the SG neurons from CFA-pretreated preparations, but because the change in synaptic responsiveness was polysynaptic and not monosynaptic it is not possible to dissect out easily what is responsible and where it is acting. Nevertheless, inflammation has been shown to result in changes in the phenotype of dorsal horn neurons, including the upregulation of NK1 receptors and alterations in dynorphin expression so that postsynaptic mechanisms may be important (Ruda et al., 1988; Noguchi et al., 1991; Schafer et al., 1993; McCarson and Krause, 1994).

Although a decrease of GABAergic and glycinergic inhibition could result in an augmentation of Aβ fiber-mediated responses in the SG, this is unlikely because we found a facilitation of Aβ

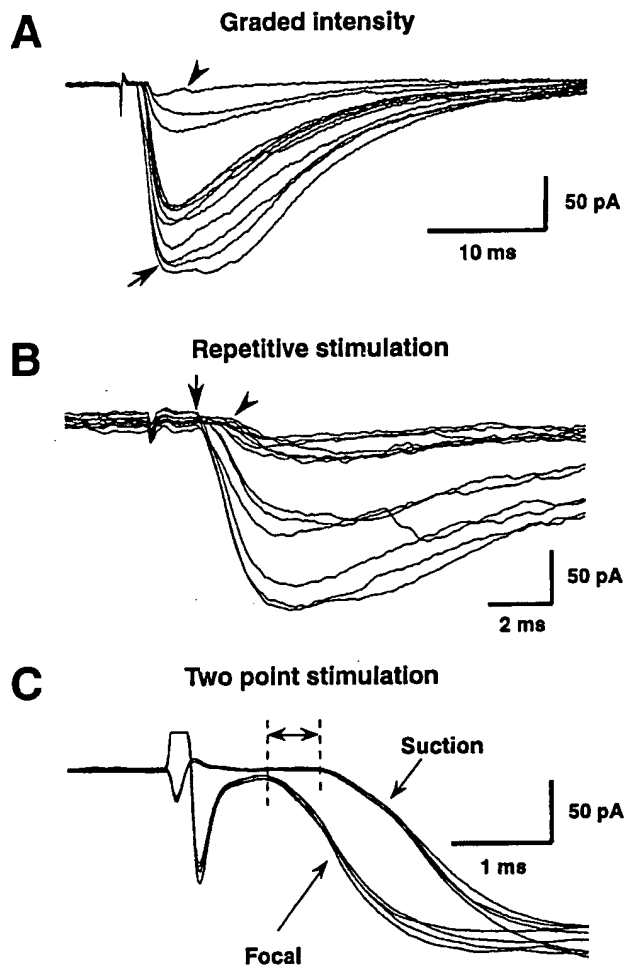

Figure 6. Aβ fiber-evoked polysynaptic EPSCs with short and variable latencies recorded in an SG cell from a slice from a rat with an inflamed hindpaw. *A*, The effect of stimulus intensity. As the intensity was increased (12–25 μA; 0.05 msec), the latency of the Aβ fiber-evoked EPSC shortened. The shortest latency was 1.6 msec at an intensity of 22–25 μA. The *arrowhead* identifies the EPSC evoked by the lowest, and the *arrow* identifies the EPSC evoked by the highest stimulus strengths. *B*, A shift in latency of the Aβ-evoked EPSCs was observed with 20 Hz repetitive stimulation at 25 μA, indicating a polysynaptic synaptic response. The *arrow* identifies the first EPSC, and the *arrowhead* identifies the last EPSC in the train. *C*, Stimulation of the dorsal root by a peripheral suction electrode and the entry zone with a focal electrode were performed to calculate the conduction velocity of fibers responsible for the evoked EPSC. Conduction velocity calculated by the difference of latencies was 32.5 m/sec (length of dorsal root, 19.5 mm).

fiber-mediated IPSCs as well as EPSCs after inflammation. We cannot exclude the possibility, however, that disinhibition occurs in laminae III or IV. This too seems unlikely, though, because both GABA and the $GABA_A$ receptor are upregulated in the dorsal horn after peripheral inflammation (Castro-Lopes et al., 1994).

After peripheral nerve injury, Aβ fibers sprout from lamina III into lamina II (Woolf et al., 1992), and Aβ fiber-mediated monosynaptic EPSCs, which are never normally observed in SG, can be detected (Okamoto et al., 1996). We have been unable, however, to detect any evidence of Aβ fiber sprouting after CFA inflammation at 48 hr (Q-P. Ma and C. Woolf, unpublished observations), which is in keeping with the lack of any monosynaptic input after this treatment.

Functional consequences of augmented Aβ input to the SG

Several studies recording from large cells in the deep dorsal horn have shown that inflammation alters receptive field size and properties (Ren et al., 1992a,b; Ren and Dubner, 1993). Synaptic input to lamina II cells is, as we show here, also modified. A recruitment of low-threshold mechanoreceptive input to nociceptive-specific neurons, including those in the superficial dorsal horn, occurs after central sensitization induced by capsaicin or mustard oil (Simone et al., 1989; Woolf et al., 1994). Central sensitization may contribute to the change in SG responsiveness to Aβ input after inflammation caused by an ongoing activity in C-fibers generated by the presence of inflammatory mediators in the inflamed tissue. Such a mechanism is unlikely, though, to be a major contributor in the present experiments, in which the sensory fibers are disconnected from the periphery, unless the inflammation-induced activity generates very long-lasting changes in membrane excitability.

The processing of sensory information in the spinal cord is dynamic, and it is this modifiability that is a major contributor to alterations in sensation after inflammation or nerve injury. The fact that an area of the spinal cord normally devoted almost exclusively to nociceptive input begins after inflammation to receive low-threshold synaptic input is a further indication of the plasticity of the system. What causes the changes and whether they contribute to inflammatory pain hypersensitivity needs now to be established.

REFERENCES

Baba H, Kohno T, Okamato M, Goldstein PA, Shimoji K, Yoshimura M (1998) Muscarinic facilitation of GABA release in substantia gelatinosa of the rat spinal dorsal horn. J Physiol (Lond) 508:83–93.

Beal JA, Bicknell HR (1985) Development and maturation of neurons in the substantia gelatinosa(SG) of the rat spinal cord. In: Development, organization and processing in somatosensory pathway (Rowe M, Willis Jr WD, eds), pp 23–30. New York: Wiley-Liss.

Bennett GJ, Abdelmoumene M, Hayashi H, Dubner R (1980) Physiology and morphology of substantia gelatinosa neurons intracellularly stained with horseradish peroxidase. J Comp Neurol 194:809–827.

Bleazard L, Hill RG, Morris R (1994) The correlation between the distribution of the NK1 receptor and the action of tachykinin agonists in the dorsal horn of the rat indicates that substance P does not have a functional role on substantia gelatinosa (lamina II) neurons. J Neurosci 14:7655–7664.

Brown AG (1981) Organization in the spinal cord: the anatomy and physiology of identified neurones. Berlin: Springer-Verlag.

Castro-Lopes JM, Tavares I, Tolle TR, Coimbra A (1994) Carragenan-induced inflammation of the hind foot provokes a rise of GABA-immunoreactive cells in the rat spinal cord that is prevented by peripheral neurectomy or neonatal capsaicin treatment. Pain 56:193–201.

Harper AA, Lawson SN (1985) Conduction velocity is related to morphological cell type in rat dorsal root ganglion neurons. J Physiol (Lond) 359:31–46.

Herrero JF, Cervero F (1996a) Changes in nociceptive reflex facilitation during carrageenan-induced arthritis. Brain Res 717:62–68.

Herrero JF, Cervero F (1996b) Supraspinal influences on the facilitation of rat nociceptive reflexes induced by carrageenan monoarthritis. Neurosci Lett 209:21–24.

Hunt SP, Pini A, Evan G (1987) Induction of c-fos-like protein in spinal cord neurones following sensory stimulation. Nature 328:632–634.

Koltzenburg M, Torebjork HE, Wahren LK (1994) Nociceptor modulated central sensitization causes mechanical hyperalgesia in acute chemogenic and chronic neuropathic pain. Brain 117:579–591.

Kumazawa T, Perl ER (1978) Excitation of marginal and substantia gelatinosa neurons in the primate spinal cord: indications of their place in dorsal horn functional organization. J Comp Neurol 177:417–434.

Levine JD, Taiwo YO (1994) Inflammatory pain. In: Textbook of pain (Wall PD, Melzack R, eds), pp 45–56. Edinburgh: Churchill Livingstone.

Light AR, Trevino DL, Perl ER (1979) Morphological features of functionally defined neurons in the marginal zone and substantia gelatinosa of the spinal dorsal horn. J Comp Neurol 186:151–172.

Lynn B, Carpenter SE (1982) Primary afferent units from the hairy skin of the rat hind limb. Brain Res 238:29–43.

Ma Q-P, Woolf CJ (1996a) Progressive tactile hypersensitivity: an inflammation-induced incremental increase in the excitability of the spinal cord. Pain 67:97–106.

Ma Q-P, Woolf CJ (1996b) Basal and touch-evoked fos-like immunoreactivity during experimental inflammation in the rat. Pain 67:307–316.

McCarson KE, Krause JE (1994) NK-1 and NK-3 type tachykinin receptor mRNA expression in the rat spinal cord dorsal horn is increased during adjuvant or formalin-induced nociception. J Neurosci 14:712–720.

Neumann S, Doubell TP, Leslie TA, Woolf CJ (1996) Inflammatory pain hypersensitivity mediated by phenotypic switch in myelinated primary sensory neurones. Nature 384:360–364.

Noguchi K, Kowalski K, Traub R, Solodkin A, Iadarola MJ, Ruda MA (1991) Dynorphin expression and fos-like immunoreactivity following inflammation induced hyperalgesia are co-localized in spinal cord neurons. Brain Res Mol Brain Res 10:227–233.

Okamoto M, Yoshimura M, Baba H, Higashi H, Shimoji K (1996) Synaptic plasticity of substantia gelatinosa neurons in the chronic pain model rat. Jpn J Physiol 46:S136.

Presley RW, Menetrey D, Levine JD, Bausbaum AI (1990) Systemic morphine suppresses noxious stimulus-evoked fos protein-like immunoreactivity in the rat spinal cord. J Neurosci 10:323–335.

Randic M, Cheng G, Kojic L (1995) k-opioid receptor agonists modulate excitatory transmission in substantia gelatinosa neurons of the rat spinal cord. J Neurosci 15:6809–6826.

Ren K, Dubner R (1993) NMDA receptor antagonists attenuate mechanical hyperalgesia in rats with unilateral inflammation of the hindpaw. Neurosci Lett 163:22–26.

Ren K, Hylden JLK, Williams GM, Ruda MA, Dubner R (1992a) The effects of a non-competitive NMDA receptor antagonist, MK- 801, on behavioural hyperalgesia and dorsal horn neuronal activity in rats with unilateral inflammation. Pain 50:331–344.

Ren K, Williams GM, Hylden JLK, Ruda MA, Dubner R (1992b) The intrathecal administration of excitatory amino acid receptor antagonists selectively attenuated carrageenan-induced behavioral hyperalgesia in rats. Eur J Pharmacol 219:235–243.

Ruda MA, Iadarola MJ, Cohen LV, Young WS, III (1988) In situ hybridization histochemistry and immunocytochemistry reveal and increase in spinal dynorphin biosynthesis in a rat model of peripheral inflammation and hyperalgesia. Proc Natl Acad Sci USA 85:622–626.

Sandkuhler J, Chen JG, Cheng G, Randic M (1997) Low-frequency stimulation of afferent Aδ-fibers induces long term depression at primary afferent synapses with substantia gelatinosa neurons in the rat. J Neurosci 17:6483–6491.

Schafer MK, Nohr D, Krause JE, Weihe E (1993) Inflammation-induced upregulation of NK1 receptor mRNA in dorsal horn neurones. NeuroReport 4:1007–1010.

Simone DA, Baumann TK, Collins JG, LaMotte RH (1989) Sensitization of cat dorsal horn neurons to innocuous mechanical stimulation after intradermal injection of capsaicin. Brain Res 486:185–189.

Stein C, Millan MJ, Herz A (1988) Unilateral inflammation of the hindpaw in rats as a model of prolonged noxious stimulation: alterations in behavior and nociceptive thresholds. Pharmacol Biochem Behav 31:445–451.

Thompson SW, King AE, Woolf CJ (1990) Activity-dependent changes in rat ventral horn neurones *in vitro*: summation of prolonged afferent evoked postsynaptic depolarizations produce a D-APV sensitive windup. Eur J Neurosci 2:638–649.

Thompson SW, Woolf CJ, Sivilotti LG (1993) Small caliber afferents produce a heterosynaptic facilitation of the synaptic responses evoked by primary afferent A fibres in the neonatal rat spinal cord *in vitro*. J Neurophysiol 69:2116–2128.

Thompson SW, Dray A, Urban L (1994) Injury-induced plasticity of spinal reflex activity: NK1 neurokinin receptor activation and enhanced A- and C-fiber mediated responses in the rat spinal cord *in vitro*. J Neurosci 14:3672–3687.

Torebjork HE, Lundberg LER, LaMotte RH (1992) Central changes in processing of mechanoreceptor input in capsaicin-induced sensory hyperalgesia in humans. J Physiol (Lond) 448:765–780.

Villiere V, McLachlan EM (1996) Electrophysiological properties of neurons in intact rat dorsal root ganglia classified by conduction velocity and action potential duration. J Neurophysiol 76:1924–1941.

Willis WD, Coggeshall RE (1991) Sensory mechanisms of the spinal cord. New York: Plenum.

Woolf CJ (1983) Evidence for a central component of post-injury pain hypersensitivity. Nature 306:686–688.

Woolf CJ (1987) Central terminations of cutaneous mechanoreceptive afferents in the rat lumbar spinal cord. J Comp Neurol 261:105–119.

Woolf CJ, Fitzgerald M (1983) The properties of neurons recorded in the superficial dorsal horn of the rat spinal cord. J Comp Neurol 221:313–328.

Woolf CJ, King AE (1990) Dynamic alterations in the cutaneous mechanoreceptive fields of dorsal horn neurons in the rat spinal cord. J Neurosci 10:2717–2726.

Woolf CJ, Shortland P, Coggeshall RE (1992) Peripheral nerve injury triggers central sprouting of myelinated afferents. Nature 355:75–77.

Woolf CJ, Shortland P, Sivilotti LG (1994) Sensitization of high mechanothreshold superficial dorsal horn and flexor motor neurons following chemosensitive primary afferent activation. Pain 58:141–155.

Yoshimura M, Jessell TM (1989) Primary afferent evoked synaptic responses and slow potential generation in rat substantia gelatinosa neurons *in vitro*. J Neurophysiol 62:96–108.

Yoshimura M, Jessell TM (1990) Amino acid-mediated EPSPs at primary afferent synapses with substantia gelatinosa neurones in the rat spinal cord. J Physiol (Lond) 430:315–335.

Yoshimura M, Nishi S (1993) Blind patch-clamp recordings from substantia gelatinosa neurons in adult rat spinal cord slices: pharmacological properties of synaptic currents. Neuroscience 53:519–526.

Yoshimura M, Nishi S (1995) Primary afferent-evoked glycine- and GABA-mediated IPSPs in substantia gelatinosa neurones in the rat spinal cord *in vitro*. J Physiol (Lond) 482:29–38.

The Journal of Neuroscience, November 1, 1997, 17(21):8476–8490

Nerve Growth Factor Treatment Increases Brain-Derived Neurotrophic Factor Selectively in TrkA-Expressing Dorsal Root Ganglion Cells and in Their Central Terminations within the Spinal Cord

G. J. Michael,[1] S. Averill,[1] A. Nitkunan,[2] M. Rattray,[3] D. L. H. Bennett[2], Q. Yan,[4] and J. V. Priestley[1]

[1]Department of Anatomy, Faculty of Basic Medical Sciences, Queen Mary and Westfield College, London 31 4NS, United Kingdom, Departments of [2]Physiology and [3]Biochemistry, United Medical and Dental Schools, St. Thomas's Hospital Medical School Campus, London SE1 7EH, United Kingdom, and [4]Amgen Inc., Amgen Centre, Thousand Oaks, California 91320-1789

Using immunocytochemistry and *in situ* hybridization, we have examined the expression of brain-derived neurotrophic factor (BDNF) and of neurotrophin receptors in dorsal root ganglion cells. In the adult rat, BDNF mRNA and protein were found mainly in the subpopulation of cells that express the nerve growth factor (NGF) receptor trkA and the neuropeptide calcitonin gene-related peptide (CGRP). NGF increased BDNF within the trkA/CGRP cells to the extent that almost 90% of trkA cells contained BDNF mRNA after intrathecal NGF treatment, and 80–90% of BDNF-expressing cells contained trkA. Non-trkA cells that expressed BDNF included some trkC cells and some small cells that labeled with the lectin *Griffonia simplicifolia* IB4, a marker for cells that do not express trks. However, very few trkB cells expressed either BDNF mRNA or protein, and NGF did not increase BDNF expression in non-trkA cells. BDNF protein was anterogradely transported both peripherally and centrally. The central transport resulted in BDNF immunoreactivity in CGRP containing terminal arbors in the dorsal horn of the spinal cord, and this immunoreactivity was increased by NGF treatment. Electron microscopic analysis revealed that the BDNF immunoreactivity was present in finely myelinated and unmyelinated axons and in axon terminals, where it was most concentrated over dense-cored vesicles.

Our data do not support an autocrine or paracrine role for BDNF within normal dorsal root ganglia, but indicate that BDNF may act as an anterograde trophic messenger. NGF levels in the periphery could influence dorsal horn neurons via release of BDNF from primary afferents.

Key words: brain-derived neurotrophic factor; mRNA; trkA; trkB; NGF; dorsal root ganglion cells; primary afferent; calcitonin gene-related peptide

Brain-derived neurotrophic factor (BDNF) is a member of a small family of related molecules termed neurotrophins, the other mammalian members being nerve growth factor (NGF), neurotrophin (NT)-3, and NT-4/5. The neurotrophins exert their effects through a family of tyrosine kinase (trk) receptors comprising trkA (selective for NGF), trkB (selective for BDNF and NT-4/5), and trkC (selective for NT-3) (for review, see Maness et al., 1994).

All three trks are expressed within adult dorsal root ganglia (McMahon et al.,1994; Kashiba et al., 1995; Wright and Snider, 1995), and all members of the neurotrophin family show retrograde transport to dorsal root ganglia from peripheral nerves (DiStefano et al., 1992; Curtis et al., 1995). BDNF, however, is unusual in being also produced by adult dorsal root ganglion (DRG) cells (Ernfors et al., 1990, 1993; Wetmore and Olson, 1995; Apfel al., 1996; Cho et al., 1997), although the role of this BDNF is not known. An autocrine role has been proposed on the basis of studies of single-neuron microcultures (Acheson et al., 1995). Alternatively, BDNF protein has been suggested to be released locally to act in a paracrine manner on trkB cells (Apfel et al., 1996); however, there is little information regarding the dorsal root ganglion (DRG) subtypes that synthesize BDNF. Two studies have recently reported that NGF increases BDNF mRNA in trkA-expressing cells (Apfel et al., 1996; Cho et al., 1997), but it is not known whether trkB or trkC cells synthesize BDNF. It is also not known how the expression of BDNF protein and/or mRNA relates to subgroups of DRG cells defined according to widely used neurochemical criteria (Hunt et al., 1992; Lawson, 1992). BDNF is axonally transported by DRG cells to their central and/or peripheral processes (Zhou and Rush, 1996), but the cell type involved is not known.

The role of BDNF in DRG cells is given added importance by the fact that BDNF synthesis is greatly increased after nerve injury (Ernfors et al., 1993). Nerve damage causes the central terminals of large-diameter DRG cells to sprout within the dorsal horn (Woolf et al., 1992), and this sprouting can be prevented by NGF treatment (Bennett et al., 1996a). The stimulus for the sprouting is not known, but it has been suggested that it might be in response to BDNF released from the terminals of small-diameter DRG cells (Mannion et al., 1996). BDNF released from primary afferents might have profound effects on both spinal cord anatomy and physiology.

Received April 23, 1997; revised July 21, 1997; accepted Aug. 12, 1997.

This work was supported by the Medical Research Council (UK) and the Wellcome Trust. We thank Professor J. M. Polak and Dr. D. O. Clary for provision of rabbit CGRP and trkA antibodies. Human recombinant NGF was a generous gift of Genentech Inc.

Correspondence should be addressed to Professor J. V. Priestley, Department of Anatomy, Faculty of Basic Medical Sciences, Queen Mary and Westfield College, Mile End Road, London E1 4NS, UK.

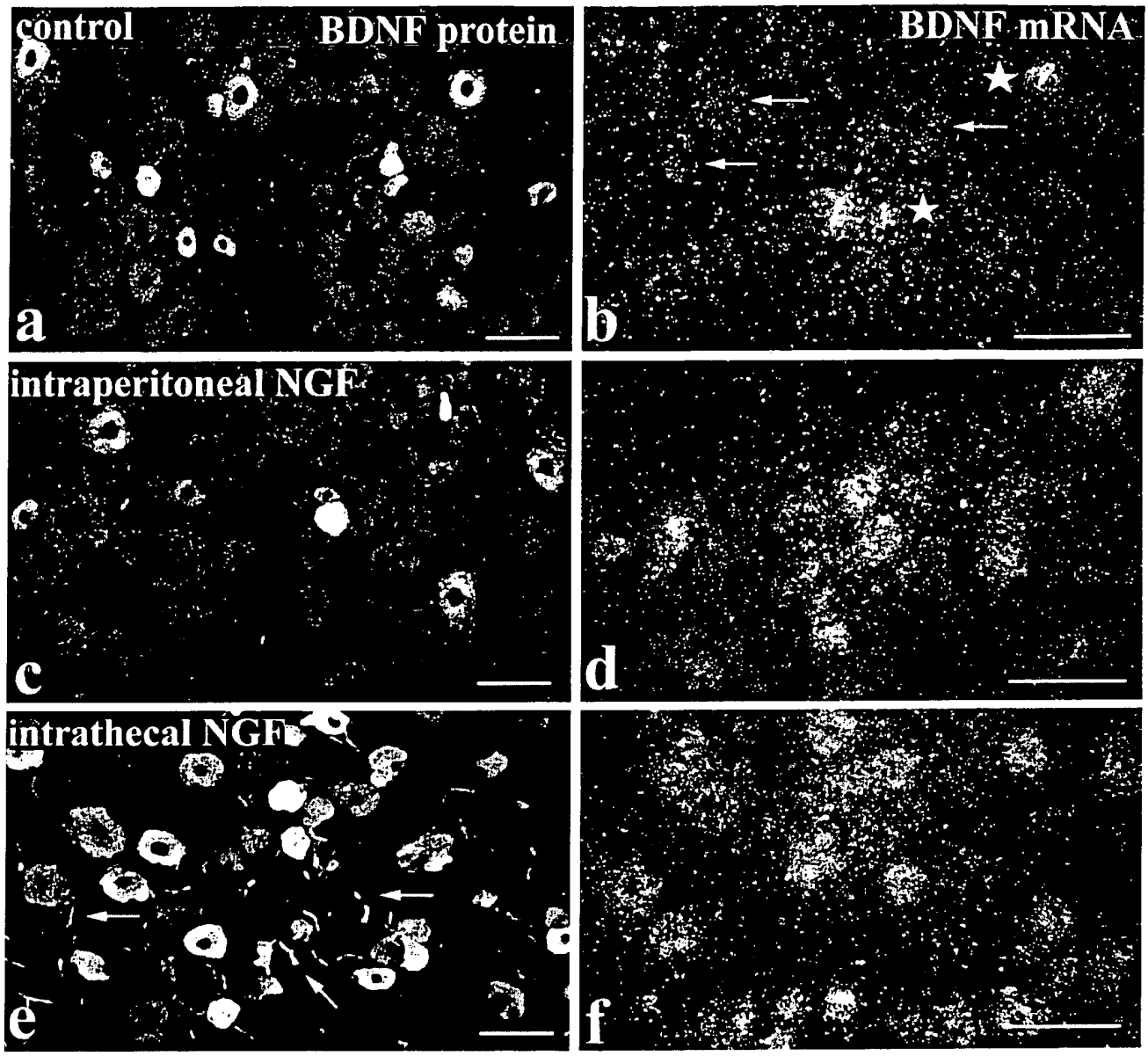

Figure 1. BDNF mRNA and protein are increased by NGF treatment. BDNF immunofluorescence (*a, c, e*) and *in situ* hybridization (*b, d, f*) in lumbar ganglia of control (*a, b*), intraperitoneal NGF-treated (*c, d*), and intrathecal NGF-treated (*e, f*) rats. BDNF immunoreactivity is present in small to medium sized DRG cells and is increased after NGF treatment. The increase is most evident after intrathecal NGF (*e*), where immunoreactivity is seen not only in a larger number of DRG cells but also in neighboring axons (*arrows*). NGF treatment also increases expression of BDNF mRNA. In control tissue (*b*), a few heavily labeled cells are seen (*stars*) together with scattered light labeling (*arrows*). The number of heavily labeled cells is increased after intraperitoneal NGF (*d*) and increased even more by intrathecal NGF (*f*). Scale bars, 100 μm.

To clarify some of these issues we have used *in situ* hybridization and immunocytochemistry to establish the DRG cell types that express BDNF and the changes that take place in response to systemic or intrathecal NGF. We have also examined axonal transport of BDNF protein, its distribution in the spinal cord, and its subcellular location within axon terminals.

A preliminary report of some of this work has been published previously in abstract form (Priestley et al., 1996).

MATERIALS AND METHODS

Tissue preparation. A total of 18 adult male Wistar rats (200–400 gm body weight) were processed for BDNF immunocytochemistry or *in situ* hybridization. Four of these had 1 mg/kg intraperitoneal injections of recombinant human NGF 13 or 24 hr before perfusion, four had intra-

Table 1. The effect of intraperitoneal NGF (IP NGF) or intrathecal NGF on the percentage of DRG cells expressing BDNF mRNA, BDNF immunoreactivity, or trkA immunoreactivity

	Control	IP NGF	Intrathecal NGF
BDNF immunoreactivity	22.3 ± 1.2% (3)	22.3 ± 3.3% (3)	40 ± 1.5% (4)**
BDNF mRNA	28.5 ± 3.3% (4)	43.7 ± 4.4% (3)*	37.8 ± 1.4% (4)*
TrkA immunoreactivity	37.8 ± 2.2% (4)	37.5 ± 2.0% (4)	42.3 ± 3.1% (3)

The figures in brackets indicate the number of animals analyzed. * indicates significantly different from controls at $p < 0.05$; ** indicates $p < 0.001$.

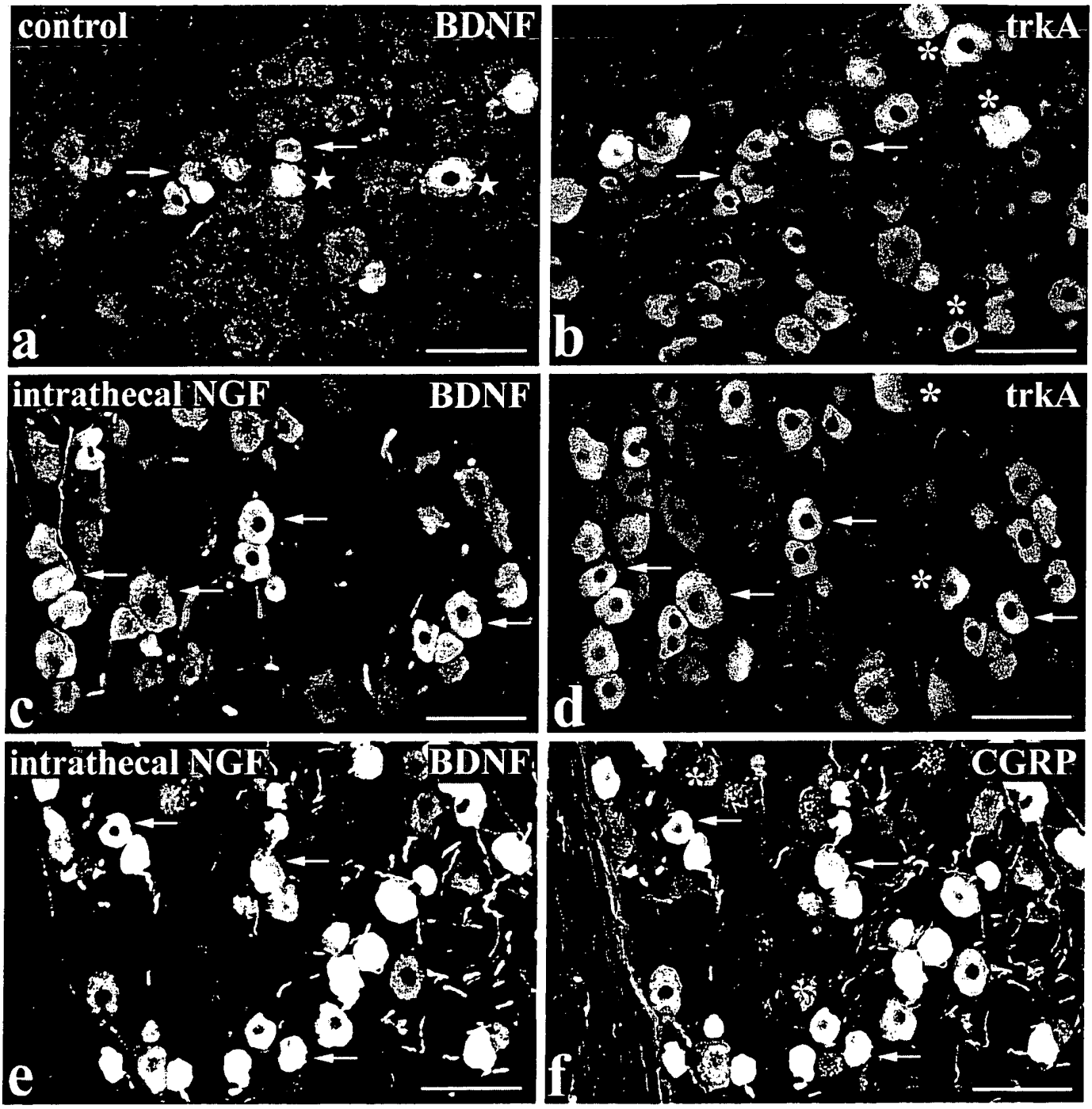

Figure 2. BDNF immunoreactivity is present in trkA/CGRP cells and is increased by NGF treatment. Double-labeling for BDNF (*a, c, e*) and either trkA (*b, d*) or CGRP (*f*) immunofluorescence in lumbar ganglia of control (*a, b*) and intrathecal NGF-treated (*c–f*) rats is shown. In both control and intrathecally treated animals, the majority of BDNF-immunoreactive DRG cells are also trkA immunoreactive (*a–d*). However, because intrathecal NGF increases the level of BDNF immunoreactivity, the number of trkA-immunoreactive cells that double-label for BDNF is increased in *c* and *d* compared with *a* and *b*. A similar situation occurs for BDNF and CGRP double-labeling, with extensive coexistence of BDNF and CGRP evident after intrathecal NGF treatment (*e, f*). *Arrows* indicate BDNF/trkA or BDNF/CGRP double-labeled cells; *asterisks* indicate cells single-labeled for trkA or CGRP; *stars* indicate cells single-labeled for BDNF. Scale bars, 100 μm.

thecal NGF, and five had unilateral ligations of dorsal roots or sciatic nerves.

Intrathecal delivery of NGF was performed basically as described previously (Bennett et al., 1996a). A laminectomy of the L5 and L6 vertebrae was performed under pentobarbitone anesthesia (Sagatal, Rhône Mérieux Ltd., UK) (40 mg/kg, i.p.). The dura was cut, and a SILASTIC tube (0.6 mm diameter) was passed intrathecally so that its tip lay over the lumbar enlargement. Alternatively, a tube was introduced through the foramen magnum and passed intrathecally to lie over the cervical cord. NGF (1 mg/ml in saline) was infused using a mini-osmotic pump (Alzet type 2002, Alza Corp., Palo Alto, CA) at a rate of 0.5 μl/hr for a period of 1–2 weeks. For ligation of dorsal roots, a laminectomy of

Table 2. The effect of intraperitoneal NGF (IP NGF) or intrathecal NGF on the percentage of BDNF-expressing DRG cells that also exhibit trkA or CGRP immunoreactivity

	Control		IP NGF		Intrathecal NGF	
	% of BDNF expressing other	% of other expressing BDNF	% of BDNF expressing other	% of other expressing BDNF	% of BDNF expressing other	% of other expressing BDNF
BDNF and trkA immunoreactivities	46% (200/434)	21% (200/931)	49% (207/421)	29% (207/721)	91% (201/221)	84% (201/268)
BDNF and CGRP immunoreactivities	68% (131/192)	20% (131/644)	44% (227/511)	21% (227/1088)	96% (322/335)	76% (322/424)
BDNF mRNA and trkA immunoreactivity	44% (301/507)	30% (301/810)	80% (900/1241)	60% (900/1311)	79% (540/685)	88% (540/603)

The figures in brackets indicate the number of cells counted.

the L2 and L3 vertebrae was performed, and the L4 and L5 roots were tied with a single or double 5/0 silk ligature. For peripheral nerve ligation, the sciatic nerve was exposed under pentobarbitone anesthesia and tied with a single or double 5/0 ligature at midthigh level. Ligation was performed on control rats and on rats that received intraperitoneal NGF 24 hr before ligation. Perfusion was performed 12–24 hr after ligation.

Rats were anesthetized with sodium pentobarbital (60 mg/kg) and perfused through the ascending aorta with 30 ml vascular rinse followed by 300 ml 4% paraformaldehyde in 0.1 M phosphate buffer. After 2.5–3.0 hr post-fixation, tissue blocks were cryoprotected in 15% sucrose, and 8–12 μm sections were cut on a cryostat. Sections were then stained using one of the following procedures: light microscopic immunocytochemistry, *in situ* hybridization, combined immunofluorescence and *in situ* hybridization, or preembedding electron microscopic immunocytochemistry.

Light microscopic immunocytochemistry. Sections were stained using standard single or dual color indirect labeled immunofluorescence or indirect tyramide signal amplification (TSA) (NEN) fluorescence procedures (Priestley, 1997). Incubations consisted of 1 hr in 10% normal serum followed by 18–36 hr in primary antibody and 3 hr in developing secondary antisera. For BDNF labeling, an affinity-purified rabbit antibody raised against recombinant human BDNF was used at 1:500 (indirect labeled procedure) or at 1:2000–1:5000 (TSA procedure). For double-labeling, this antibody was combined with one of the following: rabbit or sheep (Affiniti) CGRP polyclonal antisera (1:2000), rabbit polyclonal antiserum directed against the extracellular domain of trkA (code-labeled RTA, used at 2.5 μg/ml), or *Griffonia simplicifolia* IB4 lectin (Sigma, Poole, UK), which recognizes terminal α-galactose residues (12.5 μg/ml biotinylated IB4). The characteristics and staining specificity of all these markers have been reported previously (BDNF, Yan et al., 1997; RTA, Clary et al., 1994, Averill et al., 1995; rabbit CGRP, Merighi et al., 1988; goat CGRP and IB4, Averill et al., 1995). Controls for double-labeling included reversing the order of the primary antisera, as well as omitting the first or second primary antiserum. The two sets of antisera were applied sequentially, and this normally involved BDNF TSA followed by indirect labeled immunofluorescence. Although two primary antisera raised in rabbit were sometimes combined, nonspecific double-labeling was not observed. A similar protocol has been used by other workers (Hunyady et al., 1996; Shindler and Roth, 1996), and the lack of cross-reactivity is thought to be attributable to the fact that the TSA procedure allows the first series primary antibody to be used at a dilution that is too high to be detected by the second reagent set. Our data support this explanation. In control single-labeling using indirect labeled immunofluorescence, we were unable to visualize the BDNF antiserum at the dilutions used for the TSA procedure.

Secondary reagents used for indirect immunofluorescence included both FITC- and TRITC-labeled anti-rabbit IgG and anti-sheep IgG affinity-purified antisera (Jackson ImmunoResearch, West Grove, PA) (1:100 dilution) and 1:200 ExtrAvidin-FITC (for IB4 localization; Sigma). TSA labeling was performed using biotinylated goat anti-rabbit IgG (1:400) (Vector, Burlingame, CA) and Vectastain Elite peroxidase reagent (Vector) followed by biotinyl tyramide (NEN TSA-indirect kit) and ExtrAvidin-FITC (1:500, Sigma). After incubation in secondary reagents, sections were washed briefly in PBS and then mounted in PBS/glycerol (1:3) containing 2.5% 1,4 diazobicyclo (2,2,2) octane (antifading agent; Sigma).

In situ *hybridization.* Oligonucleotide probes complementary to bases 273–306 of the rat BDNF sequence (Timmusk et al., 1993), bases 124–157 of the rat trkA sequence (Meakin et al., 1992), bases 2213–2246 of the rat trkB sequence (Middlemas et al., 1991), and bases 1099–1132 of the rat trkC sequence (Valenzuela et al., 1993) were synthesized (Genosys) and then hybridized to cryostat sections using standard procedures (Michael and Priestley, 1995, 1996a). The trkB probe was directed against a portion of the tyrosine kinase domain and designed only to recognize full length receptors. The probes were labeled at the 3′ end with ^{35}S-dATP (Dupont NEN, Wilmington, DE) and terminal transferase (Promega, Madison, WI) to specific activities of ~5000 Ci/mmol. Sections were acetylated in 0.25 M acetic anhydride/0.1 M triethanolamine for 10 min, dehydrated in ethanols (70–100%), and delipidated with chloroform. Hybridizations were performed overnight at 37°C using probe concentrations of 2 nM. Hybridization buffer consisted of 4× SSC (1× SSC = 150 mM sodium chloride, 15 mM sodium citrate, pH 7.0), 50% deionized formamide, 0.04% Ficoll-400, 0.04% polyvinylpyrrolidone, 0.04% bovine serum albumin, 10% dextran sulfate, 0.1% SDS, 20 mM dithiothreitol (DTT), 20 μg/ml yeast tRNA, 100 μg/ml sheared salmon sperm DNA, and 10 μg/ml poly adenylate.

After hybridization, sections received two (15 min) washes at room temperature (RT) in 2× SSC, two at 50°C in 1× SSC, and one at 50°C in 0.2× SSC. Sections were washed an additional 2 hr at RT in 1× SSC, dehydrated through ethanols, dipped in autoradiographic emulsion (Amersham LM1), and exposed for 4–8 weeks. After development, slides were counterstained with toluidine blue, dehydrated, and coverslipped.

In situ *hybridization combined with immunofluorescence.* Immunofluorescence was followed by oligonucleotide *in situ* hybridization, as described previously (Priestley et al., 1993; Michael and Priestley, 1996b). Standard indirect immunofluorescence was performed as described above, except that antisera were diluted in diethylpyrocarbonate-treated PBS containing 0.5–5 mM DTT and 100 U/ml RNasin (Promega) in addition to 0.2% Triton X-100. After they were immunostained, sections were processed as for single BDNF *in situ* hybridization, except that developed sections were mounted in PBS/glycerol instead of being toluidine blue-counterstained and dehydrated. Silver grains in PBS/glycerol mounted sections were visualized using epipolarized illumination (Priestley et al., 1993).

Pre-embedding electron microscopic immunocytochemistry. Four animals were perfused with 4% paraformaldehyde, 0.1% glutaraldehyde in 0.1 M phosphate buffer and processed for electron microscopic immunocytochemistry using standard preembedding procedures (Priestley et al., 1992). The spinal cord was dissected out, post-fixed 2.5 hr in the same fixative, and immersed in PBS. Sections (40 μm) were cut using a vibratome (Oxford) and pretreated with 1% sodium borohydride in PBS for 30 min before they were immunostained. Sections were incubated for 30 min in 10% normal goat serum and then transferred to BDNF polyclonal antibody (1:1000) for 12 hr at 4°C. Primary antibody was subsequently revealed using 1:400 biotinylated goat anti-rabbit IgG (Vector) and Vectastain Elite peroxidase reagent (Vector). Sections were then developed with a solution containing 0.05% 3,3′-diaminobenzidine, 0.04% $(NH_4)_2SO_4.NiSO_4$, and 0.01% H_2O_2 in 0.1 M phosphate buffer, pH 7.3. Unless stated otherwise, incubations were performed at RT, and antisera were diluted in PBS. Stained sections were then contrasted in OsO_4 (1%) and uranyl acetate (1%), dehydrated, and flat-embedded in Durcupan (Fluka, Buchs,

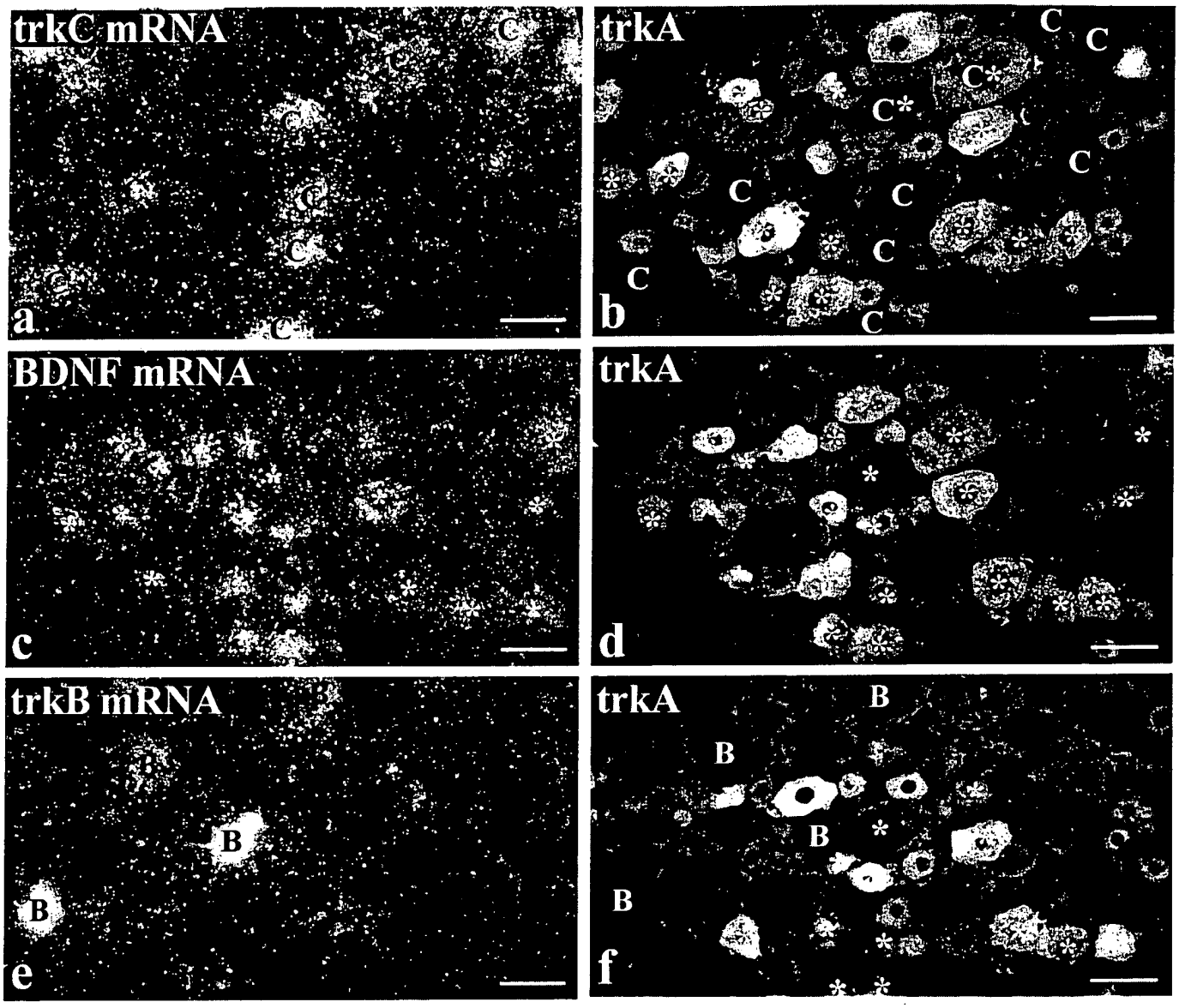

Figure 3. BDNF mRNA is expressed by numerous trkA cells but by few trkB or trkC cells. Intraperitoneal NGF treatment is shown. *a*, *c*, and *e* show three serial sections processed for trkC (*a*), BDNF (*c*), and trkB (*e*) mRNAs using *in situ* hybridization. Each section was also immunostained for trkA (*b*, *d*, *f*). Comparison of *c* and *d* shows that the majority of cells labeled for BDNF mRNA (*asterisks*) are also trkA immunoreactive. Those BDNF-labeled cells that are visible in the serial sections (*a*, *b*, *e*, *f*) are marked by *asterisks* in *b* and *f*. Comparison of *a* and *b* shows that the majority of trkC-labeled cells (marked *C*) do not express BDNF mRNA. However, two BDNF/trkC double-labeled cells are visible in *b*, one of which is trkA immunoreactive. Comparison of *e* and *f* allows the distribution of DRG cells that express trkB (marked *B*) and BDNF (*asterisks*) to be compared. They seem to form two discrete populations, and no double-labeled cells are visible. Scale bars, 50 μm.

Switzerland). After light microscopic examination, areas of interest were processed further for electron microscopy.

Imaging and quantitation. Sections were viewed on a Leica epifluorescence microscope using N2 (TRITC), L3 (FITC), and polarization filter blocks combined with bright-field and/or dark-field illumination. Immunostaining and *in situ* hybridization were documented by photography using Ilford T-MAX film. Photographs were printed by hand or were generated digitally by scanning 35 mm negatives using a Nikon LS-1000 at 900–1300 pixels/inch, by composing using Adobe Photoshop, and by printing on a Sony UP-D8800 graphics printer at 300 pixels/inch. Gray levels were stretched to optimize contrast, but images were not filtered or otherwise manipulated.

The proportion of BDNF-expressing DRG cells was determined by counting the number of immunoreactive and nonimmunoreactive neuronal profiles in sections of DRG. In double-labeled sections, the percentage of BDNF-expressing cells expressing a second marker was assessed by switching between FITC, TRITC, and/or polarization filter blocks. At least 250 labeled DRG cells were examined for each marker and counted on randomly chosen DRG sections. With use of Visilog image analysis software, the cell size and level of expression of BDNF mRNA were assessed in trkA immunoreactive and immunonegative DRG cells using previously described methodology (Priestley et al., 1991). Images were captured directly off the microscope at 25× magnification using a Grundig FA87 digital camera with integrating framestore. Cells were then outlined manually using a computer mouse, and the area within each cell that was occupied by silver grains was calculated. At least 200 cells of each type were counted. The amount of BDNF immunostaining in lamina II of the spinal cord was also quantified, basically as described previously (Bennett el al., 1996a). Images were captured as above and thresholded to reveal

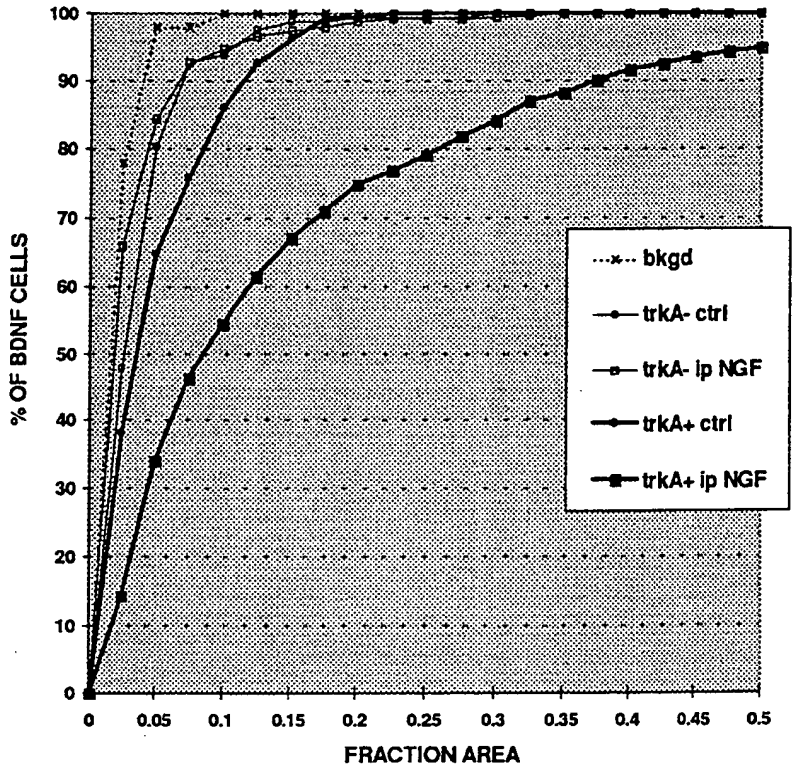

Figure 4. NGF increases BDNF mRNA expression only in trkA-immunoreactive cells as shown in Q sum plot of BDNF mRNA expression in trkA-immunoreactive (trkA+) and trkA-nonimmunoreactive (trkA−) lumbar DRG cells in control (*ctrl*) and intraperitoneal NGF-treated (*ip NGF*) animals. BDNF expression was quantified by measuring the fraction of the cell body (*FRACTION AREA*) that was covered by silver grains. Note that intraperitoneal NGF does not change the level of BDNF expression in BDNF-labeled but trkA-nonimmunoreactive cells. In contrast intraperitoneal NGF greatly increases BDNF expression in trkA immunoreactive cells, and even in control animals these cells show higher labeling than the trkA nonimmunoreactive population. *bkgd* indicates the level of background labeling in control and NGF-treated animals.

Table 3. The percentage of BDNF mRNA expressing DRG cells that also exhibit trkB mRNA, trkC mRNA, or IB4 labeling

	% of BDNF expressing other		% of other expressing BDNF	
BDNF and trkB mRNAs	1% (2/175)		2.4% (2/83)	
	trkA immunoreactive	not trkA immunoreactive	trkA immunoreactive	not trkA immunoreactive
BDNF and trkC mRNAs	8% (13/166)	7% (11/166)	10% (13/133)	8% (11/133)
BDNF mRNA and IB4 labelling	34% (71/208)	15% (31/208)	32% (71/221)	14% (31/221)

Intraperitoneal NGF treatment.

BDNF terminals, the threshold level being kept constant for both control and NGF-treated animals. Several 27 × 27 μm measuring boxes were placed over each image, and the area within each box that was occupied by immunostained terminals was calculated; 120–240 areas were sampled for each animal.

RESULTS

NGF effects on BDNF protein and BDNF mRNA in lumbar ganglia

In lumbar ganglia of control rats, BDNF immunoreactivity was evident in DRG cells and occasional axons. The quality of staining, however, varied between animals, depending on the immunocytochemical staining method. Thus few cells were stained using indirect immunofluorescence, whereas good TSA fluorescence preparations (Fig. 1*a*) showed staining in ~22% of DRG cells. Rats treated with intraperitoneal NGF showed a similar quality and range of BNDF immunostaining but little change in the number of immunoreactive DRG cells (Fig. 1*c*, Table 1). In contrast, ganglia from animals treated intrathecally with NGF showed abundant and robust BDNF immunostaining (Fig. 1*e*). As many as 40% of DRG cells showed immunoreactivity (Table 1), together with numerous axons. In all types of preparation, staining was confined to DRG cells and adjoining axons. Thus there was no indication of staining within satellite cells or Schwann cells.

In situ hybridization for BDNF mRNA showed a pattern of staining similar to that observed for BDNF protein. Thus a few heavily labeled DRG cells were observed in control animals together with numerous cells showing labeling slightly above background (Fig. 1*b*). The intraperitoneal NGF-treated animals (Fig. 1*d*) and the intrathecally treated animals (Fig. 1*f*) both showed increased labeling compared with controls. However, the total number of labeled cells increased only slightly (Table 1), suggesting that the increased *in situ* hybridization labeling represented mainly an increase in grain density per cell.

Relationship between BDNF expression and trkA expression in lumbar ganglia

The NGF effects were characterized further by combining BDNF immunocytochemistry with immunofluorescence for trkA or CGRP. BDNF immunoreactivity was present mainly in trkA cells, but the extent of double-labeling varied according to the type of NGF treatment (Fig. 2*a–d*, Table 2). For example, the percentage of trkA-immunoreactive cells that were BDNF immunoreactive increased from 21% in controls (Fig. 2*a,b*) to 84% after intrathecal NGF (Fig. 2*c,d*). NGF also increased the double-

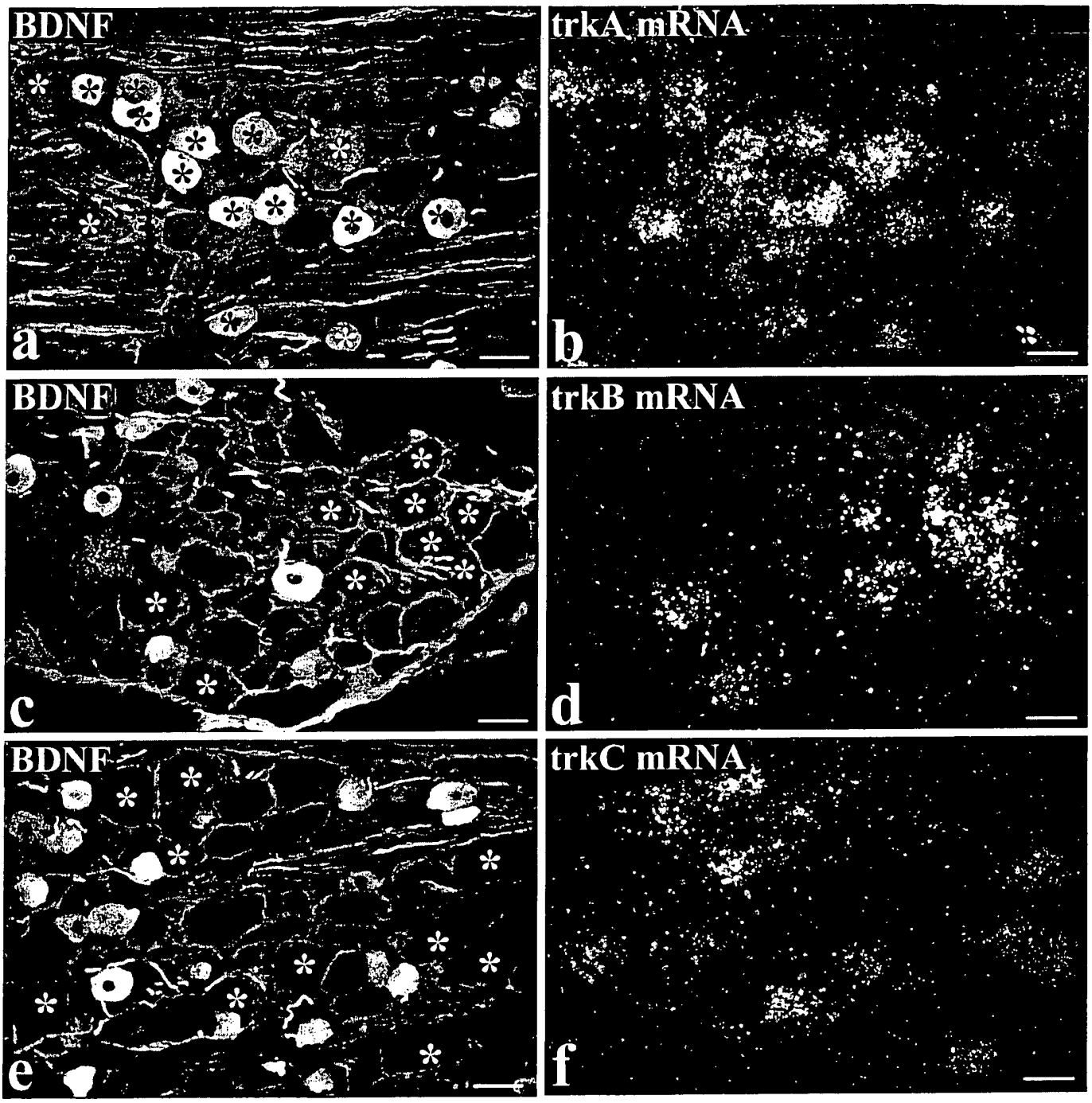

Figure 5. Intrathecal NGF treatment. BDNF immunoreactivity is present in numerous trkA cells but in few trkB or trkC cells. *a–f* show preparations double-labeled for BDNF immunoreactivity (*a, c, e*) and either trkA (*b*), trkB (*d*), or trkC (*f*) *in situ* hybridization. The *asterisks* indicate the location of trk-expressing cells, revealed by the *in situ* hybridization autoradiograms. Many BDNF-immunoreactive cells show trkA labeling (*a, b*), but the trkB- and trkC-expressing cells are distinct from the BDNF-immunoreactive ones. Scale bars, 50 μm.

labeling in terms of the percentage of BDNF cells that were trkA immunoreactive (Table 2). Very similar results were obtained for CGRP, consistent with previous studies showing that CGRP labels broadly the same DRG subpopulation as trkA (Averill et al., 1995). Thus extensive coexistence of BDNF and CGRP immunoreactivities was observed (Fig. 2*e,f*), and this coexistence varied according to the type of NGF treatment in the same way as the trkA/BDNF coexistence (Table 2).

To determine whether the BDNF protein observed in trkA/CGRP cells was locally synthesized, BDNF *in situ* hybridization was also combined with trkA immunofluorescence (Fig. 3*c,d*, Table 2). Just as with BDNF protein, extensive overlap was observed between BDNF mRNA and trkA, and the degree of coexistence increased with NGF treatment. Thus 30% of trkA-immunoreactive cells expressed BDNF mRNA in controls, whereas this figure increased to 88% after intrathecal NGF (Ta-

Table 4. The percentage of BDNF-immunoreactive DRG cells that also express trkA, trkB, or trkC mRNA

	% of BDNF expressing trk	% of trk expressing BDNF
BDNF and trkA mRNA	85% (583/684)	82% (583/706)
BDNF and trkB mRNA	2.5% (18/708)	9.5% (18/179)
BDNF and trkC mRNA	6% (53/842)	13% (53/399)

Intrathecal NGF treatment. The figures in brackets indicate the number of cells counted.

ble 2). To exclude the possibility that these changes in BDNF/trkA double-labeling were caused by changes in trkA expression, the effect of NGF on trkA immunoreactivity was also examined. The percentage of DRG cells that were trkA immunoreactive was not significantly affected by NGF treatment (Table 1).

Judged on the basis of either immunocytochemistry or *in situ* hybridization, a proportion of BDNF-expressing cells were not trkA immunoreactive (Figs. 2, 3; Table 2). Image analysis of preparations double-labeled for BDNF *in situ* hybridization and trkA immunofluorescence was performed to quantify the extent of labeling for BDNF mRNA in the trkA-immunoreactive and trkA-nonimmunoreactive cells and to quantify the effect of intraperitoneal NGF on the two populations. Consistent with the impression given by micrographs (e.g., Fig. 3*c,d*), this analysis showed that the trkA-immunoreactive cells had greater labeling for BDNF mRNA than the non-trkA cells and that intraperitoneal NGF greatly increased the degree of labeling in the trkA subpopulation (Fig. 4). In addition, it revealed that intraperitoneal NGF had no effect on the degree of BDNF mRNA labeling in the non-trkA cell population (Fig. 4) and had no effect on the cell-size distribution of the trkA subpopulation (data not shown).

Relationship between BDNF expression and trkB or trkC expression in lumbar ganglia

To determine the relationship between BDNF and trkB or trkC expression, two different methods of double-labeling were performed. The first method was used for animals treated with intraperitoneal NGF. Serial sections were processed for trkC, BDNF, and trkB *in situ* hybridization, and each section was also immunostained for trkA (Fig. 3). The trkA/BDNF double-labeled sections were also stained with the lectin *Griffonia simplicifolia* IB4, a marker that has been proposed to mainly label DRG cells that do not express any known trk (Averill et al., 1995; Molliver et al., 1995; Silos-Santiago et al., 1995). This approach allowed us to determine whether BDNF-synthesizing cells belonged to the trkB, trkC, or non-trk (IB4) populations and also revealed whether labeled cells coexpressed trkA. A small overlap was seen between BDNF and both the trkC and IB4 populations. Thus 15% of BDNF mRNA-expressing cells were labeled for trkC mRNA, of which half were also trkA immunoreactive (Fig. 3*a,b*, Table 3). In addition, 49% of BDNF mRNA-expressing cells showed IB4 labeling (not illustrated), with approximately two thirds of these also trkA immunoreactive (Table 3). In contrast to trkC or IB4, however, there was virtually no overlap between BDNF mRNA and trkB. Only 1% of BDNF mRNA-expressing cells were also labeled for trkB mRNA (Fig. 3*e,f*, Table 3).

The second method of double-labeling was applied to animals treated intrathecally with NGF and involved BDNF immunofluorescence combined with trkA, trkB, or trkC *in situ* hybridization (Fig. 5). This allowed a direct analysis of whether BDNF protein was present in trkB- or trkC-expressing cells, as well as providing an additional assessment of the degree of BDNF/trkA coexpression. Consistent with the other labeling methods, a high percentage of trkA mRNA-expressing cells were BDNF immunoreactive (82%) (Table 4). A small percentage of BDNF-immunoreactive cells expressed trkC mRNA (6%), and an even smaller percentage expressed trkB (3%) (Table 4).

BDNF axonal transport

To determine whether BDNF was axonally transported to or from lumbar dorsal root ganglia, BDNF immunoreactivity was examined at the site of dorsal root (Fig. 6*a,b*) and sciatic (Fig. 6*e,f*) ligations. The accumulation of BDNF immunoreactivity was compared with that of trkA (Fig. 6*c,d*) and CGRP (Fig. 6*g,h*) immunoreactivities. In dorsal roots, BDNF transport seemed to be mainly anterograde. BDNF immunoreactivity accumulated predominantly proximal to a dorsal root ligation (i.e., the DRG side). In contrast, both anterograde and retrograde transport of trkA was evident. TrkA immunoreactivity accumulated both proximal and distal to the ligation but with greater accumulation proximal rather than distal (Fig. 6*a–d*). In the sciatic nerve, both anterograde and retrograde transport of BDNF were detected. BDNF immunoreactivity accumulated both proximal (DRG side) and distal to a sciatic ligation (Fig. 6*e,f*). The proximal accumulation was generally greater than that distally, and on both sides of the ligation the majority of BDNF-immunoreactive axons were also CGRP immunoreactive (Fig. 6*e–h*). The BDNF accumulation in dorsal roots and sciatic nerve was greater after intraperitoneal NGF than in control animals, and in the case of double ligatures no accumulation was seen in the isolated portion of nerve between the ligatures (not illustrated). The footpad and dorsal surface of the foot were examined for peripherally transported BDNF. Immunoreactivity was present but was confined to light staining of fiber bundles in the dermis and of isolated axons in the epidermis (not illustrated).

BDNF immunoreactivity in the spinal cord

BDNF immunoreactivity was examined in the lumbar cord of control (Fig. 7*a,b*), intraperitoneal NGF-treated (not illustrated), and intrathecal NGF-treated (Figs. 7*c,d*) animals. BDNF immunoreactive axons and terminals were observed mainly in the central projections of small diameter primary afferents. Terminals were particularly abundant in the superficial dorsal horn (laminae I, II) (Figs. 7*a,c*), in patches in deep dorsal horn (Fig. 7*c,e*), and dorsolateral to the central canal (Fig. 7*g*). In all of these regions, BDNF showed extensive coexistence with CGRP (Figs. 7*e–h*), such that BDNF-immunoreactive axons that lacked CGRP immunoreactivity were rarely observed. In contrast to CGRP, BDNF-immunoreactive terminals did not coexist with IB4 (not illustrated). As with the staining in DRG, the extent of BDNF immunoreactivity in spinal cord varied, depending on whether animals had been treated with NGF. Control and intrathecal NGF-treated animals were easily distinguished. After intrathecal NGF, BDNF-immunoreactive terminals were more abundant (compare Fig. 7, *a* and *c*), and more extensive coexistence with CGRP was seen. After intrathecal delivery of NGF to the cervical cord, the BDNF immunoreactivity in primary afferents was so intense that it was possible to trace axons from the ganglion into the dorsal horn (Fig. 8). Staining in intraperitoneal NGF-treated animals was not as great as in intrathecally treated animals, and there was significant interanimal variability. In general, however,

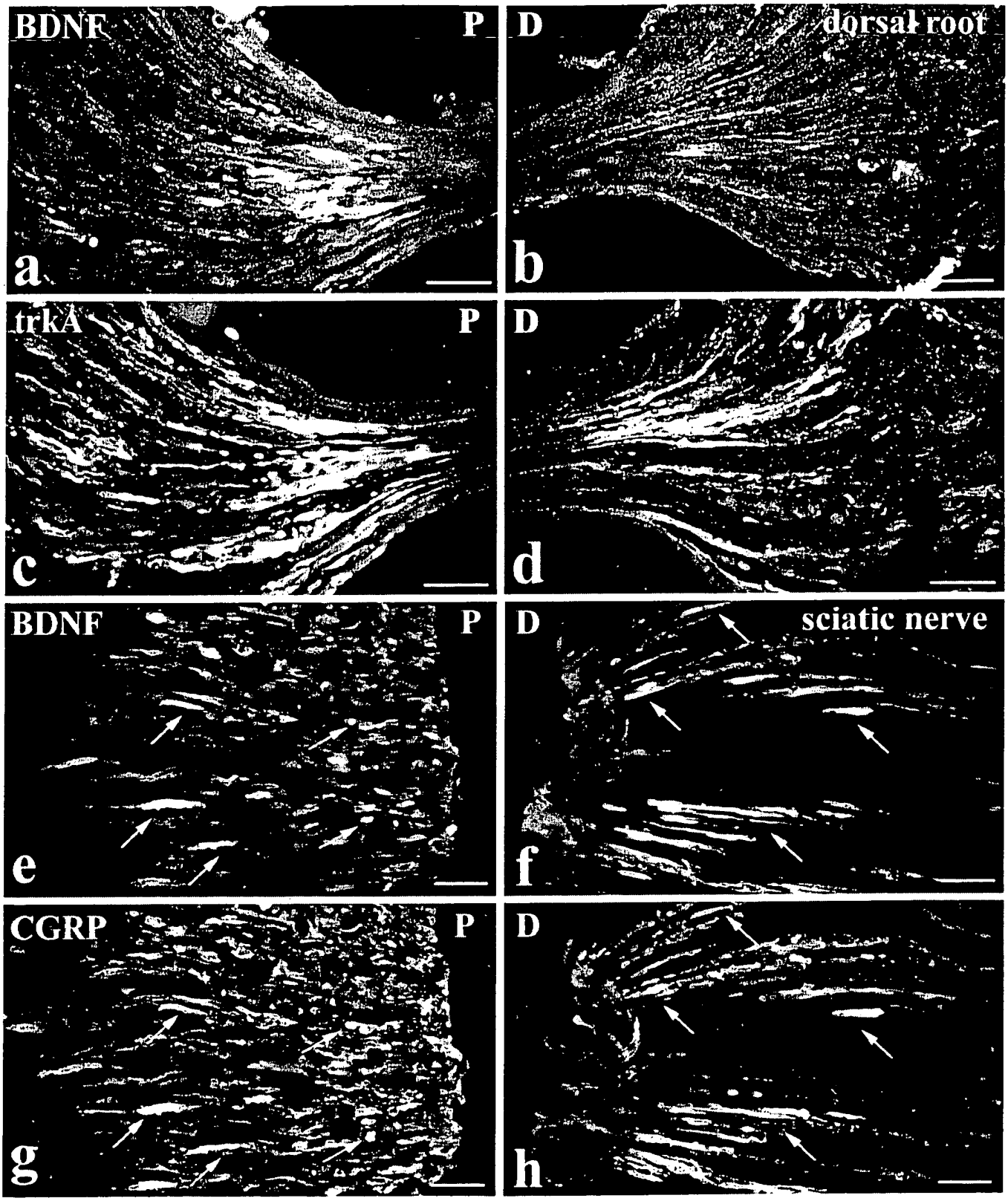

Figure 6. Intraperitoneal NGF treatment. BDNF is anterogradely transported. BDNF (*a, b, e, f*), trkA (*c, d*), and CGRP (*g, h*) immunoreactivity proximal (*P: a, c, e, g*) and distal (*D: b, d, f, h*) to lumbar dorsal root (*a–d*) or sciatic nerve (*e–h*) ligations are shown. At a dorsal root ligation, both BDNF (*a*) and trkA (*c*) accumulate proximal to the ligation (i.e., the DRG side). Distal to the ligation, trkA immunoreactivity accumulates (*d*) but only occasional BDNF-immunoreactive axons are visible (*b*). At a sciatic nerve ligation, BDNF accumulates both proximal (*e*) and distal (*f*) to the ligation. CGRP shows a similar accumulation (*g, h*), and double-staining reveals that the BDNF-immunoreactive axons are also CGRP immunoreactive (*arrows* indicate double-labeled axons). Scale bars, 50 μm.

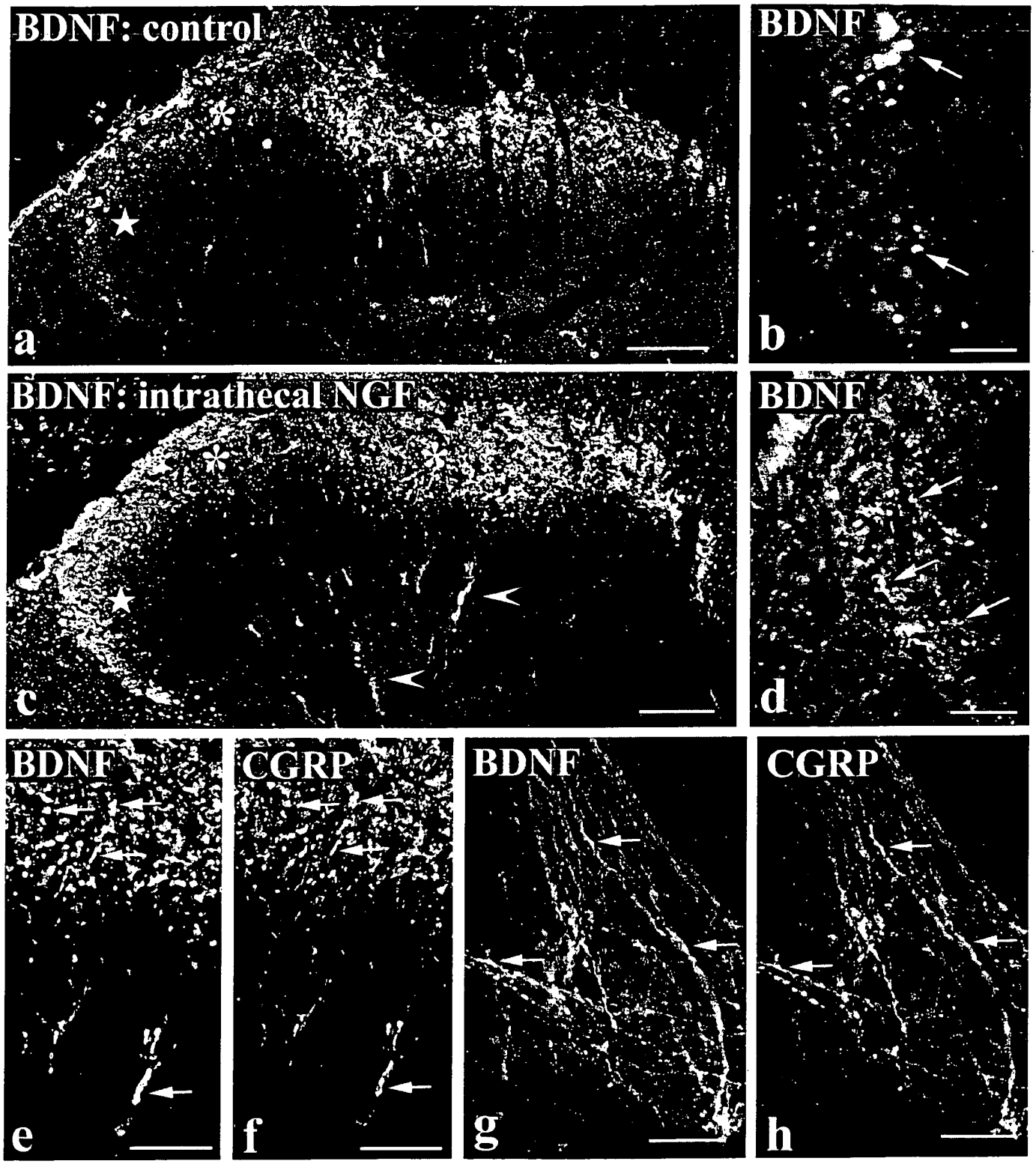

Figure 7. BDNF immunoreactivity in the spinal cord is increased by NGF treatment and is present in CGRP-immunoreactive axons. *a–d* show BDNF immunofluorescence in the dorsal horn of control tissue (*a*, *b*) and after intrathecal NGF treatment (*c*, *d*). BDNF immunoreactivity in laminae I and II (*asterisks* in *a* and *c*) and in deep dorsal horn (*arrowheads* in *c*) is increased by NGF. The increase is particularly striking in lateral lamina II (*stars* in *a* and *c*), and this region is shown at high magnification in *b* and *d*. Immunoreactive axons (*arrows* in *b* and *d*) are more abundant after NGF treatment. *e–h*, Double-labeling showing extensive coexistence of BDNF (*e*, *g*) and CGRP (*f*, *h*) after intrathecal NGF treatment. In the dorsal horn (*e*, *f*) and in lamina X dorsolateral to the aqueduct (*g*, *h*), numerous double-labeled axons and varicosities (*arrows*) are visible. Scale bars: *a*, *c*, 100 μm; *b*, *d*, 25 μm; *e–h*, 50 μm.

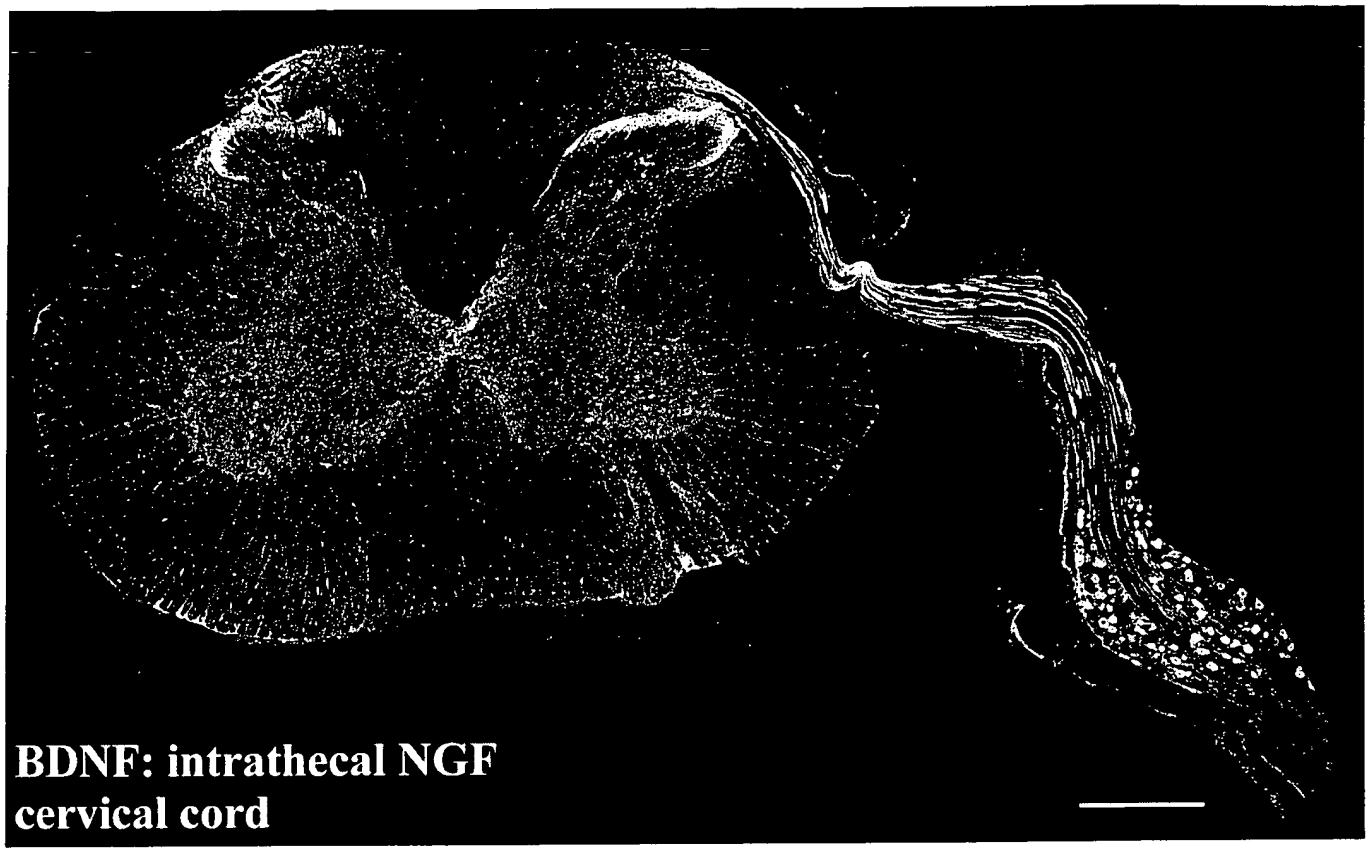

Figure 8. Photomontage of a transverse section showing the cervical spinal cord and attached DRG of an animal treated intrathecally with NGF via an upper cervical cannula. BDNF protein is transported by DRG cells along their central processes and into the spinal cord. BDNF levels have increased to such an extent that immunoreactive axons can be traced from DRG cells, along a dorsal root and into the dorsal horn of the spinal cord. Scale bar, 250 μm.

it seemed to be slightly greater than in controls, and this was confirmed by image analysis. The mean staining level of BDNF-immunoreactive terminals in lamina II of intraperitoneal NGF-treated animals was twice that obtained in control animals.

Ultrastructural localization of BDNF immunoreactivity in the dorsal horn

Immunoreactive unmyelinated axons (Fig. 9*b*), finely myelinated axons (Fig. 9*c*), and axon terminals (Fig. 9*a*) were observed in lamina II. Immunoreactive terminals included characteristic sinuous terminals that made asymmetric synapses and displayed an electron-dense axoplasm containing several large dense-cored vesicles and numerous agranular vesicles (Fig. 9*a*). In heavily stained terminals, the immunoreaction deposit filled the axoplasm and covered dense-cored vesicles and the membranes of agranular vesicles. In lightly stained terminals, the reaction deposit had a more restricted distribution and seemed to be concentrated over a subpopulation of dense-cored vesicles (Fig. 9*c*).

DISCUSSION

In this study we have shown that trkA-expressing DRG cells synthesize BDNF and anterogradely transport it to axon terminals within the spinal cord. BDNF levels are modulated by NGF, with intrathecally administered NGF having much more potent effects than systemic NGF. In addition we have shown that a small number of DRG cells that do not express trkA also synthesize BDNF but that BDNF mRNA in these cells is not increased by NGF. Such cells include trkC cells and cells that do not express any of the trks, but very few trkB cells. The expression of BDNF protein in DRG cells matches very closely the expression of BDNF mRNA. These results have profound implications for our understanding of BDNF function in sensory neurons.

DRG subgroups that synthesize BDNF

Previous studies have described BDNF mRNA (Ernfors et al., 1990, 1993; Wetmore and Olson, 1995; Apfel et al., 1996; Cho et al., 1997) or protein (Wetmore and Olson, 1995; Zhou and Rush, 1996) in adult rat DRG cells, and two studies have recently reported that some cells expressing BDNF mRNA also express trkA mRNA (Apfel et al., 1996; Cho et al., 1997). We have extended these studies by fully characterizing the expression of both BDNF mRNA and protein in relation to all of the trk-expressing subpopulations of DRG cells.

Our results show that BDNF is synthesized by several different DRG subtypes, but the biggest contribution comes from cells that express trkA and the neuropeptide CGRP (Fig. 10). TrkA-immunoreactive cells in control animals have higher levels of BDNF mRNA than non-trkA-immunoreactive cells, and after intrathecal NGF, BDNF and trkA/CGRP identify virtually identical populations. Of the BDNF-expressing cells, 80–90% belong to the trkA group, and almost 90% of trkA cells express BDNF mRNA. This close correspondence between BDNF and the trkA/CGRP group is echoed in the spinal cord, where BDNF immunoreactivity in both control and NGF-treated animals is confined to CGRP containing primary afferents. BDNF is absent

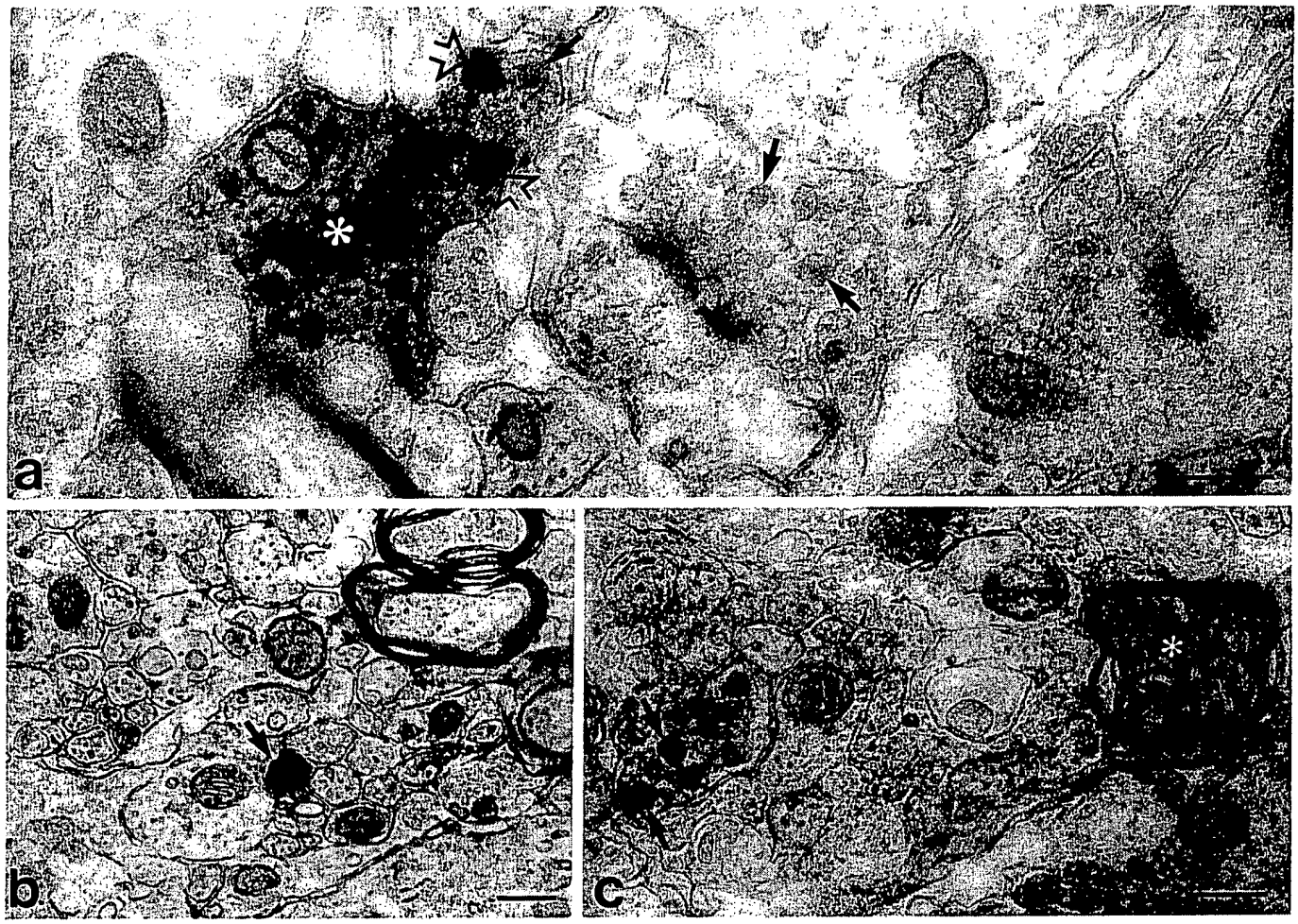

Figure 9. Preembedding ultrastructural immunocytochemistry showing BDNF immunoreactivity in axons (*b, c*) and an axon terminal (*a*) in lamina II of the lumbar spinal cord. *a*, An immunoreactive terminal (*asterisk*) shows heavy staining over a region packed with small agranular vesicles and over individual large dense-cored vesicles (*open arrows*). *Arrows* indicate dense-cored vesicles in an adjoining unstained terminal. *b*, A heavily stained unmyelinated axon (*arrow*) is visible among a group of similar, but unstained, axons. *c*, An immunostained preterminal axon and an immunostained finely myelinated axon (*asterisk*) are visible. The preterminal axon shows staining exclusively over large dense-cored vesicles (*arrows*). Scale bars, 0.25 μm.

from the termination zones of large-diameter afferents and of IB4-labeled afferents, consistent with our data showing that relatively few trkC- or IB4-labeled cells express BDNF mRNA. However, the fact that these cell types express some BDNF may be significant. NGF increases BDNF expression selectively in trkA-immunoreactive cells (discussed below), but it is possible that BDNF in the non-trkA population is affected by other factors. For example, BDNF expression in DRG cells is increased by nerve damage (Ernfors et al., 1993), and we have shown recently that this occurs at least partly in trkC cells (Averill et al., 1997). *In vitro*, a BDNF autocrine loop has been shown to mediate the survival of a subpopulation of adult DRG cells (Acheson et al., 1995). Our results, however, indicate that *in vivo* there is very little coexistence of BDNF and trkB mRNAs. Only 1% of cells expressing BDNF mRNA also expressed trkB, and only 2% of trkB cells contained BDNF mRNA. The simplest interpretation of this data is that an autocrine loop does not occur in control or NGF-supplemented adult animals. However, our data do not rule out the possibility that an autocrine loop occurs in certain circumstances. Axonal damage may upregulate BDNF in trkB cells, or BDNF may support survival of trkA cells in some way that does not involve trkB. We also cannot exclude the possibility that some BDNF cells express trkB at levels below our detection threshold. Consistent with other recent studies (Kashiba et al., 1995; Wright and Snider, 1995; McMahon et al., 1997), we observed minimal overlap between trkA and trkB cells (Fig. 10). However, extensive overlap of trkA and trkB has been described (McMahon et al., 1994) and may be attributable to low-level trkB expression in some trkA cells.

Our preparations showed good BDNF immunostaining, with BDNF mRNA and protein generally in rather similar numbers and types of cells. After NGF, BDNF mRNA was observed in more cells than BDNF protein. However, this probably simply reflects the fact that a greater increase in BDNF expression was needed to bring cells above the detection threshold for immunocytochemistry than for *in situ* hybridization. In contrast to the extensive coexistence of BDNF and trkA, we observed very little BDNF protein in trkB cells. Only 10% of trkB-labeled cells showed BDNF immunoreactivity. This is a surprising result, given that target-derived BDNF is thought to be axonally transported by trkB-expressing DRG cells (DiStefano et al., 1992). However, our studies of BDNF axonal transport support our

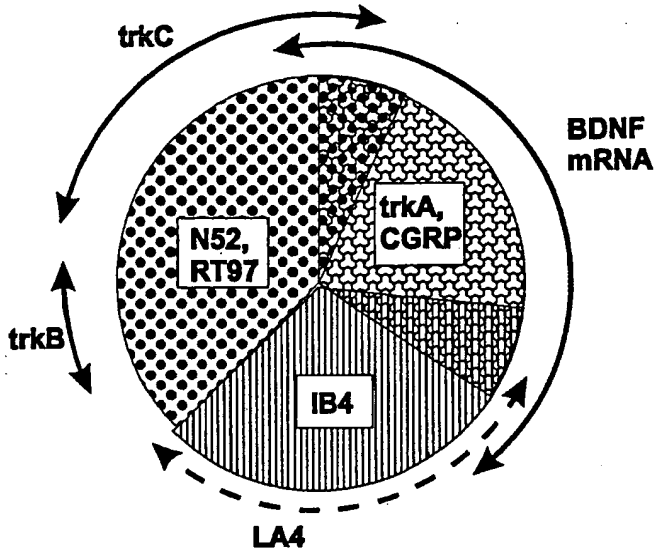

Figure 10. Pie chart summarizing the relationship between BDNF and trk expression in neurochemically defined DRG subclasses. DRG neurons can be divided broadly into large-diameter cells, which innervate low-threshold mechanoreceptors, and small-diameter cells, which innervate mainly nociceptors. BDNF mRNA is expressed by the subpopulation of small cells that contain the neuropeptide CGRP and the NGF receptor trkA. Small cells that do not express any trk receptor, and that can be labeled using the lectin *Griffonia simplicifolia* IB4 or the monoclonal antibody LA4, mainly do not express BDNF. With the exception of those trkC cells that coexpress trkA, BDNF mRNA is also largely not expressed by trkB or trkC cells. TrkC and trkB are present mainly in large-diameter cells, which can be identified using the neurofilament antisera N52 or RT97. BDNF is constitutively expressed in the cell types illustrated, but expression in trkA cells is increased further by NGF treatment.

localization data in indicating that there is little retrograde BDNF transport. BDNF immunoreactivity accumulated distal to a sciatic ligation but showed extensive colocalization with CGRP, implying that it represents mainly recycling of anterogradely transported protein. BDNF may be present in trkB cells at levels below our detection threshold, but if so it must be at levels that are much lower than those that occur in trkA cells. It thus seems that most BDNF protein in DRG cells is synthesized locally, with target-derived BDNF making only a small contribution.

Upregulation of BDNF by NGF and its functional consequences

In addition to detecting BDNF protein within trkA/CGRP immunoreactive DRG cell bodies, we observed that BDNF in these cells is (1) anterogradely transported along both their central and peripheral processes and (2) present in the spinal cord in all their terminal fields, and that (3) immunoreactivity is concentrated over dense-cored vesicles. Biochemical studies have recently shown that BDNF in cortex is enriched in a vesicular fraction of synaptosomes (Fawcett et al., 1997). Our ultrastructural results are consistent with this work and indicate that dense-cored vesicles are likely to be the primary site of BDNF storage. NGF treatment led to a massive increase of both mRNA and protein, with increased anterograde transport to central terminals. Anterograde transport of BDNF into the dorsal horn has also recently been reported by Zhou and Rush (1996), although the cell type responsible was not identified. Transport and axodendritic transfer of exogenous NT-3 has recently been reported in the developing visual system (von Bartheld et al., 1996), and BDNF-immunoreactive terminals have been described in various CNS regions (Kawamoto et al., 1996; Conner et al., 1997; Yan et al., 1997), suggesting that anterograde transport may be widespread. Goodman and colleagues (1996) have demonstrated that BDNF in cultured cells colocalizes with the secretory granule marker chromogranin A and is released from hippocampal dendrites by a regulated pathway dependent on extracellular calcium (Goodman et al., 1996). BDNF release has not been demonstrated *in vivo*, but our observations make it highly likely that BDNF can be released from primary afferent terminals in the dorsal horn.

Our data on the effects of NGF are broadly in agreement with the recent study of Apfel and colleagues (1996) in showing that NGF upregulates BDNF mRNA in trkA-expressing DRG cells; however, there are some differences of detail. They observed no effect of chronic NGF treatment and interpreted the BDNF response as an acute reaction. In contrast, we observed that a 2 week intrathecal NGF infusion had a much more potent effect, indicating not only the increased efficacy of the intrathecal route but also that the BDNF increase is maintained. Primary afferents presumably normally respond to NGF, acting at their peripheral processes, and so the intrathecal route is not like the situation *in vivo*. However, effects after intrathecal and intraperitoneal or local nerve application are qualitatively similar (this study; also see Verge et al., 1996), suggesting that the intrathecal route is appropriate for examining DRG responses to trophic factors.

Apfel and colleagues (1996) also report that BDNF mRNA is increased in non-trkA expressing cells and interpret this as a paracrine interaction. In contrast we saw no change in this cell group. Quantitative analysis of the increase in BDNF mRNA after NGF indicated that it was restricted to the trkA-immunoreactive subpopulation, as might be expected if it involves direct activation of trkA receptors. A similar analysis was not performed after intrathecal NGF, so we cannot exclude the possibility that the intrathecal route increased BDNF in some non-trkA cells. However, the extensive overlap observed between trkA and BDNF after intrathecal NGF makes it unlikely.

Our data thus support neither an autocrine nor a paracrine role for BDNF within DRG, but do support a role as an anterograde trophic messenger. Such a role has been described in late embryonic development (Robinson et al., 1996) and may be maintained, or adapted, into adult life. Many trkA-expressing DRG cells are nociceptive, and increased NGF in inflammation has both acute and chronic effects on pain processing (McMahon, 1996; Woolf, 1996). We have shown that exogenous NGF increases BDNF expression in trkA cells, and Cho et al. (1997) have recently shown that similar changes take place after peripheral inflammation. BDNF released from primary afferent terminals may therefore play a key role in chronic pain states by modulating dorsal horn activity in various ways. Full length trkB receptors are present in the dorsal horn (G. J. Michael and J. V. Priestley, unpublished observations), and BDNF applied to the spinal cord increases c-*fos* and nitric oxide synthase in dorsal horn neurons (Bennett et al., 1996b). BDNF may also have effects on spinal cord anatomy and on expression of neurotransmitter receptors. These possibilities are being investigated.

REFERENCES

Acheson A, Conover JC, Fandl JP, DeChlara TM, Russell M, Thadani A, Squinto SP, Yancopoulos GD, Lindsay RM (1995) A BDNF

autocrine loop in adult sensory neurons prevents cell death. Nature 374:450–453.

Apfel SC, Wright DE, Wiideman AM, Dormia C, Snider WD, Kessler JA (1996) Nerve growth-factor regulates the expression of brain-derived neurotrophic factor messenger RNA in the peripheral nervous system. Mol Cell Neurosci 7:134–142.

Averill S, McMahon SB, Clary DO, Reichardt LF, Priestley JV (1995) Immunocytochemical localization of trkA receptors in chemically identified subgroups of adult rat sensory neurons. Eur J Neurosci 7:1484–1494.

Averill S, Michael GJ, Shortland PJ, Priestley JV (1997) BDNF increases in large diameter dorsal root ganglion cells and in their central projections following peripheral axotomy. Soc Neurosci Abstr 23:134.8.

Bennett DLH, French J, Priestley JV, McMahon SB (1996a) NGF but not NT-3 or BDNF prevents the A fibre sprouting into lamina II of the spinal cord that occurs following axotomy. Mol Cell Neurosci 8:211–220.

Bennett DLH, French JS, Priestley JV, McMahon SB (1996b) The effects of BDNF on c-fos and NOS expression in dorsal horn neurones of the adult rat spinal cord. Soc Neurosci Abstr 22:396.15.

Cho HJ, Kim SY, Park MJ, Kim DS, Kim JK, Chu MY (1997) Expression of mRNA for brain-derived neurotrophic factor in the dorsal root ganglion following peripheral inflammation. Brain Res 749:358–362.

Clary DO, Weskamp G, Austin LAR, Reichardt LF (1994) TrkA cross-linking mimics neuronal responses to nerve growth factor. Mol Biol Cell 5:549–563.

Conner JM, Lauterborn JC, Yan Q, Gall CM, Varon S (1997) Distribution of brain-derived neurotrophic factor (BDNF) protein and mRNA in the normal adult rat CNS: evidence for anterograde axonal transport. J Neurosci 17:2295–2313.

Curtis R, Adryan KM, Stark JL, Park JS, Compton DL, Weskamp G, Huber LJ, Chao MV, Jaenisch R, Lee KF, Lindsay RM, DiStefano PS (1995) Differential role of the low-affinity neurotrophin receptor (p75) in retrograde axonal-transport of the neurotrophins. Neuron 14:1201–1211.

DiStefano PS, Friedman B, Radziejewski C, Alexander C, Boland P, Schick CM, Lindsay RM, Wiegand SJ (1992) The neurotrophins BDNF, NT-3, and NGF display distinct patterns of retrograde axonal transport in peripheral and central neurons. Neuron 8:983–993.

Ernfors P, Wetmore C, Olson L, Persson H (1990) Identification of cells in rat brain and peripheral tissues expressing mRNA for members of the nerve growth factor family. Neuron 5:511–526.

Ernfors P, Rosario CM, Merlio JP, Grant G, Aldskogius H, Persson H (1993) Expression of mRNAs for neurotrophin receptors in the dorsal root ganglion and spinal cord during development and following peripheral or central axotomy. Mol Brain Res 17:217–226.

Fawcett JP, Aloyz R, Mclean JH, Pareek S, Miller FD, McPherson PS, Murphy RA (1997) Detection of brain-derived neurotrophic factor in a vesicular fraction of brain synaptosomes. J Biol Chem 272: 8837–8840.

Goodman LJ, Valverde J, Lim F, Geschwind MD, Federoff HJ, Geller AI, Hefti F (1996) Regulated release and polarized localization of brain-derived neurotrophic factor in hippocampal neurons. Mol Cell Neurosci 7:222–238.

Hunt SP, Mantyh PW, Priestley JV (1992) The organization of biochemically characterized sensory neurons. In: Sensory neurons. Diversity, development, and plasticity (Scott SA, ed), pp 60–76. New York: Oxford UP.

Hunyady B, Krempels K, Harta G, Mezey E (1996) Immunohistochemical signal amplification by catalyzed reporter deposition and its application in double immunostaining. J Histochem Cytochem 44:1353–1362.

Kashiba H, Noguchi K, Ueda Y, Senba E (1995) Coexpression of trk family members and low-affinity neurotrophin receptors in rat dorsal-root ganglion neurons. Mol Brain Res 30:158–164.

Kawamoto Y, Nakamura S, Nakano S, Oka N, Akiguchi I, Kimura J (1996) Immunohistochemical localization of brain-derived neurotrophic factor in adult rat brain. Neuroscience 74:1209–1226.

Lawson SN (1992) Morphological and biochemical cell types of sensory neurons. In: Sensory neurons. Diversity, development, and plasticity (Scott SA, ed), pp 27–59. New York: Oxford UP.

Maness LM, Kastin AJ, Weber JT, Banks WA, Beckman BS, Zadina JE (1994) The neurotrophins and their receptors: structure, function, and neuropathology. Neurosci Biobehav Rev 18:143–159.

Mannion RJ, Doubell TP, Coggeshall RE, Woolf CJ (1996) Collateral sprouting of uninjured primary afferent A-fibers into the superficial dorsal horn of the adult rat spinal cord after topical capsaicin treatment to the sciatic-nerve. J Neurosci 16:5189–5195.

McMahon SB (1996) NGF as a mediator of inflammatory pain. Philos Trans R Soc Lond [Biol] 351:431–440.

McMahon SB, Armanini MP, Ling LH, Phillips HS (1994) Expression and coexpression of trk receptors in subpopulations of adult primary sensory neurons projecting to identified peripheral targets. Neuron 12:1161–1171.

McMahon SB, Bennett DLH, Michael GJ, Priestley JV (1997) Neurotrophic factors and pain. In: Progress in pain research and management, Vol 8 (Jensen TS, Turner JA, Wiesenfeld-Hallin Z, eds). Seattle: IASP Press, in press.

Meakin SO, Suter U, Drinkwater CC, Welcher AA, Shooter EM (1992) The rat trk protooncogene product exhibits properties characteristic of the slow nerve growth factor receptor. Proc Natl Acad Sci USA 89:2374–2378.

Merighi A, Polak JM, Gibson SJ, Gulbenkian S, Valentino KL, Peirone SM (1988) Ultrastructural studies on calcitonin gene-related peptide-immunoreactive, tachykinin-immunoreactive and somatostatin-immunoreactive neurons in rat dorsal root ganglia: evidence for the colocalization of different peptides in single secretory granules. Cell Tissue Res 254:101–109.

Michael GJ, Priestley JV (1995) Expression of GAP-43 messenger-RNA in preganglionic sympathetic neurons of the adult rat spinal cord. NeuroReport 7:338–342.

Michael GJ, Priestley JV (1996a) Expression of trkA and p75 low affinity nerve growth factor receptors in the adrenal gland. NeuroReport 7:1617–1622.

Michael GJ, Priestley JV (1996b) Combined immunocytochemistry and in situ hybridization. In: In situ hybridization techniques for the brain (Henderson Z, ed), pp. 111–118. Chichester: Wiley.

Middlemas DS, Lindberg RA, Hunter T (1991) TrkB, a neural receptor protein-tyrosine kinase: evidence for a full-length and two truncated receptors. Mol Cell Biol 11:143–153.

Molliver DC, Radeke MJ, Feinstein SC, Snider WD (1995) Presence or absence of trkA protein distinguishes subsets of small sensory neurons with unique cytochemical characteristics and dorsal horn projections. J Comp Neurol 361:404–416.

Priestley JV (1997) Immunocytochemical techniques for the study of the nervous system. In: Neurochemistry: a practical approach, 2nd ed (Bachelard H, Turner A, eds), pp 71–120. Oxford: Oxford UP.

Priestley JV, Réthelyi M, Lund PK (1991) Semi-quantitative analysis of somatostatin mRNA distribution in the rat central nervous system using in situ hybridization. J Chem Neuroanat 4:131–153.

Priestley JV, Alvarez FJ, Averill S (1992) Pre-embedding electron microscopic immunocytochemistry. In: Electron microscopic immunocytochemistry (Polak JM, Priestley JV, eds), pp 89–121. Oxford: Oxford UP.

Priestley JV, Wotherspoon G, Savery D, Averill S, Rattray M (1993) A combined in situ hybridization and immunofluorescence procedure allowing visualisation of peptide mRNA and serotonin in single sections. J Neurosci Methods 48:99–110.

Priestley JV, Michael GJ, Averill S, Nitkunan A, Wotherspoon G, Rattray M, Bennett DLH, Yan Q, McMahon SB (1996) NGF treatment increases BDNF expression in trkA immunoreactive dorsal root ganglion cells and in their central terminations within the spinal cord. Soc Neurosci Abstr 22:223.8.

Robinson M, Bujbello A, Davies AM (1996) Paracrine interactions of BDNF involving NGF-dependent embryonic sensory neurons. Mol Cell Neurosci 7:143–151.

Shindler KS, Roth KA (1996) Double immunofluorescent staining using two unconjugated primary antisera raised in the same species. J Histochem Cytochem 44:1331–1335.

Silos-Santiago I, Molliver DC, Ozaki S, Smeyne RJ, Fagan AM, Barbacid M, Snider WD (1995) Non-trkA-expressing small DRG neurons are lost in trkA deficient mice. J Neurosci 15:5929–5942.

Timmusk T, Palm K, Metsis M, Reintam T, Paalme V, Saarma M, Persson H (1993) Multiple promoters direct tissue-specific expression of the rat BDNF gene. Neuron 10:475–489.

Valenzuela DM, Maisonpierre PC, Glass DJ, Rojas E, Nunez L, Kong Y, Stitt TN, Ip NY, Yancopoulos GD (1993) Alternative forms of rat TrkC with different functional capabilities. Neuron 10:963–974.

Verge VMK, Gratto KA, Karchewski LA, Richardson PM (1996) Neu-

rotrophins and nerve injury. Philos Trans R Soc Lond [Biol] 351:423–430.

von Bartheld CS, Byers MR, Williams R, Bothwell M (1996) Anterograde transport of neurotrophins and axodendritic transfer in the developing visual system. Nature 379:830–833.

Wetmore C, Olson L (1995) Neuronal and nonneuronal expression of neurotrophins and their receptors in sensory and sympathetic ganglia suggest new intercellular trophic interactions. J Comp Neurol 353:143–159.

Woolf CJ (1996) Phenotypic modification of primary sensory neurons: the role of nerve growth factor in the production of persistent pain. Philos Trans R Soc Lond [Biol] 351:441–448.

Woolf CJ, Shortland P, Coggeshall RE (1992) Peripheral nerve injury triggers central sprouting of myelinated afferents. Nature 355:75–78.

Wright DE, Snider WD (1995) Neurotrophin receptor mRNA expression defines distinct populations of neurons in rat dorsal root ganglia. J Comp Neurol 351:329–338.

Yan Q, Rosenfeld RD, Matheson CR, Hawkins N, Lopez OT, Bennett L, Welcher AA (1997) Expression of brain-derived neurotrophic factor (BDNF) protein in the adult rat central nervous system. Neuroscience 78:431–448.

Zhou XF, Rush RA (1996) Endogenous brain-derived neurotrophic factor is anterogradely transported in primary sensory neurons. Neuroscience 74:945–951.

This Page is Inserted by IFW Indexing and Scanning Operations and is not part of the Official Record

BEST AVAILABLE IMAGES

Defective images within this document are accurate representations of the original documents submitted by the applicant.

Defects in the images include but are not limited to the items checked:

- ☑ BLACK BORDERS
- ☐ IMAGE CUT OFF AT TOP, BOTTOM OR SIDES
- ☐ FADED TEXT OR DRAWING
- ☐ BLURRED OR ILLEGIBLE TEXT OR DRAWING
- ☐ SKEWED/SLANTED IMAGES
- ☐ COLOR OR BLACK AND WHITE PHOTOGRAPHS
- ☐ GRAY SCALE DOCUMENTS
- ☑ LINES OR MARKS ON ORIGINAL DOCUMENT
- ☐ REFERENCE(S) OR EXHIBIT(S) SUBMITTED ARE POOR QUALITY
- ☐ OTHER: _____

IMAGES ARE BEST AVAILABLE COPY.
As rescanning these documents will not correct the image problems checked, please do not report these problems to the IFW Image Problem Mailbox.